Influence of a cyclic and dynamic loading history on dynamic properties of dry sand, part I: cyclic and dynamic torsional prestraining

T. Wichtmann [i)], Th. Triantafyllidis

Institute of Soil Mechanics and Foundation Engineering, Ruhr-University Bochum, Universitätsstrasse 150, 44801 Bochum, Germany

Abstract

Initial fabric of a soil induced by its cyclic strain history is an important parameter together with the void ratio, state of stress and amplitude in respect to further accumulation of deformations under drained cyclic loading. It is of importance for the further deformation prediction to determine the initial fabric of the grain skeleton or the cyclic loading history of the soil. An attempt is made within this paper to correlate small strain stiffness of non-cohesive soil with its cyclic loading history. The results of performed cyclic and dynamic torsional tests show that small strain shear modulus is only moderately affected by cyclic prestraining even if high amplitudes are applied. A signature of prestraining history is observed in the tests since the sand memorizes its prestraining amplitude and the number of applied cycles.

Key words: resonant column tests; dynamic soil properties; small strain stiffness; shear modulus; damping ratio; fabric; cyclic prestraining; dynamic prestraining; memory of sand

1 Introduction

The prediction of settlements under cyclic loading under drained conditions has gained in importance during the last decades of years. New high speed transport systems (e.g. Transrapid, ICE, TGV) have been developed, which transmit cyclic loads to the subsoil and whose serviceability is very sensitive to differential settlements. Another example of growing importance is the cyclic soil-structure interaction of wind power plants. Although the need for the estimation or prediction of settlements of cyclically loaded soil has grown, there exists little experimental data on the deformation behaviour of soils under very high numbers (i.e. several 10,000 up to several millions) of load cycles. Furthermore only a few constitutive models for cyclic loading with high numbers of load cycles can be found in the literature. The studies presented in this work are part of a research project with the aim to develop a reliable constitutive model for cyclically loaded sand.

From drained cyclic triaxial tests it has become obvious that knowing the actual void ratio of the sand, its average state of stress and the shear strain amplitude caused by cyclic loading is not sufficient in order to predict the accumulated deformations due to further cyclic loading. Fig. 1 shows the development of void ratio in three cyclic triaxial tests with identical average state of stress (mean pressure $p = (\sigma_1 + 2\sigma_3)/3$ and deviatoric stress $q = \sigma_1 - \sigma_3$), identical vertical stress amplitude $\Delta\sigma_1$ and different initial void ratios e_0 or different strain history. It can be seen from Fig. 1 that the rate of densification $\dot{e} = \partial e/\partial N$ differs although the average state of stress and the cyclic amplitude as well as the void ratio are the same (as pointed out by the horizontal line in Fig. 1). The rate depends on the number of load cycles already applied to the specimen, i.e. it depends on its cyclic loading history. Therefore for the prediction of expected settlements in situ due to cyclic loading the initial condition of the existing soil i.e. its cyclic loading history must be known.

Due to its cyclic loading history the fabric of a soil (i.e. number, orientation and shape of particle contacts) as well as the distribution of interparticle forces are changed. With increasing number of cycles the interparticle contacts are changed in such a way that they accomodate the applied cyclic loads without large strain accumulation. A comparison of the soil's actual fabric with the fabric of a freshly deposited or re-

[i)] Corresponding author. Tel.: 0(49)234/3226080; Fax: 0(49)234/3214150

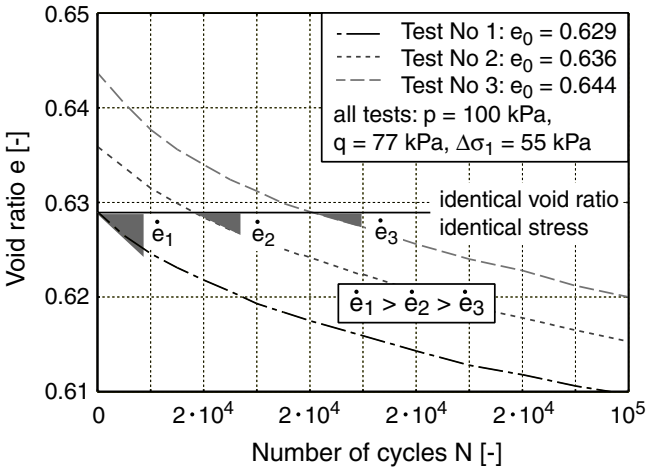

Fig. 1: Void ratio reduction in three cyclic triaxial tests with identical average stress (p = 100 kPa, q = 77 kPa) and identical vertical stress amplitude $\Delta\sigma_1$ = 55 kPa but different initial void ratios e_0

moulded soil could provide a measure of its loading history. The fabric of a soil can hardly be determined by direct methods and therefore indirect methods have to be used. One of those indirect methods is the measurement of soil parameters in the range of small strains using dynamic measurement techniques. Those small strain parameters are the compression (v_p) and shear wave velocity (v_s) and the correlated small strain stiffnesses (E_{s0}, G_0). The hypothesis is made, that changes in the soil fabric lead to a change in the small strain behaviour of the soil and this change of small strain soil parameters (also referenced as dynamic soil parameters) could be observed by means of dynamic measurement techniques.

In order to verify or disapprove this assumption series of dynamic laboratory tests on soil specimens were performed. In these experiments the development of dynamic soil properties of dry sand during cyclic and dynamic loading was studied. In one test series a dynamic torsional loading with a very high number of strain cycles was applied to specimens in the resonant column device. The development of small strain shear modulus was observed as well as the change of shear modulus and damping ratio at higher shear strains. In order to investigate the influence of the homogeneity of the shear strain distribution over the specimen's full cross section similar tests were conducted with hollow cylinder specimens in a second test series. In a third series of tests hollow cylinder specimens were cyclically prestrained in a torsional shear device. In this device higher shear strains could be applied in comparison to the first two test series in the resonant column device. After cyclic prestraining the dynamic soil properties of the specimens were determined in the resonant column device and compared with the values of non-prestrained specimens. The results of these three test series are presented in this paper.

Further test series with axial cyclic preloading and simultaneous measurement of the development of dynamic soil properties are presented in [1].

2 Review of previous work

The results of test series concerning the change of dynamic soil properties due to a cyclic or dynamic loading history that could be found in the literature are somewhat contradictory.

Drnevich and Richart [2] studied the influence of a dynamic torsional prestraining of hollow cylinder specimens on shear modulus and damping ratio in the resonant column device. The tests were performed on dry medium sand. Under a constant confining pressure the shear strain amplitude γ was increased towards a value $\gamma_{\mathrm{prestrain}}$, which was held constant during the following prestraining in the resonant frequency of the specimen. After a given number of strain cycles had been applied to the specimens the shear strain amplitude was reduced towards small values and after that it was increased again towards $\gamma_{\mathrm{prestrain}}$. During this re-increase the values of shear modulus were measured resulting in the curve $G(\gamma)$. After the prestraining amplitude $\gamma_{\mathrm{prestrain}}$ was reached again, the next package of strain cycles was applied. This procedure of decreasing and re-increasing shear strain amplitude was repeated after given numbers of cycles. Accordingly the development of the shear modulus at small strains G_0 as well as the change of $G(\gamma)$ with increasing number of strain cycles could be observed. It was found that no change of dynamic properties took place under shear strain amplitudes lower than 10^{-4}. This was true for all examined densities and pressures. Prestraining with $\gamma_{\mathrm{prestrain}} > 10^{-4}$ caused a significant increase of specimens' shear stiffness. Fig. 2 generated from data presented in [2] shows that at some combinations of density, confining pressure and prestraining amplitude the increase of small strain shear stiffness due to prestraining was found to lie even in the range of 300 % after 22 million applied strain cycles. The shear modulus at the prestraining amplitude $\mathrm{G}(\gamma_{\mathrm{prestrain}})$ was found to be almost unchanged. Drnevich and Richart [2] stated that at higher confining pressures the increase of small strain shear modulus was higher too. Although a significant increase in small strain shear modulus was obtained, the void ratio of the specimens was almost not affected during the torsional prestraining. Drnevich and Richart also found the damping ratio to grow due to cyclic prestraining and explained the increase of stiffness with the abrasion effects at particle contacts.

Specimens of loose and dense sand were subjected to dynamic torsional loading with a shear strain ampli-

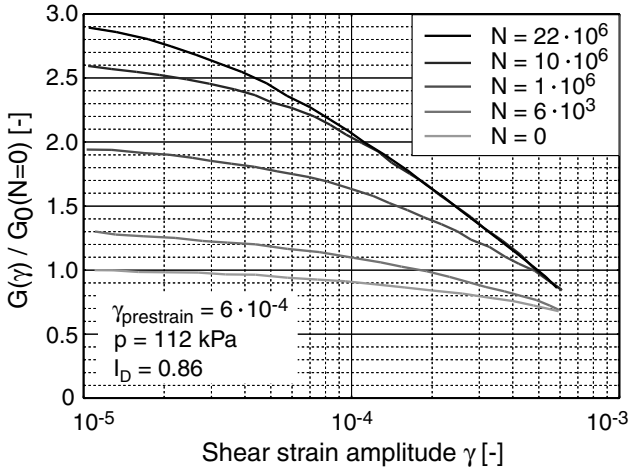

Fig. 2: Stiffness increase due to torsional prestraining after Drnevich and Richart [2]

tude $\gamma_{\text{prestrain}} = 1.4 \cdot 10^{-4}$ under a confining pressure of 80 kPa by Shen et al. [3]. After the application of a definite number of strain cycles the small strain shear modulus was measured using the method of free vibration. Chen et al. reported an increase of G_0 during 50,000 strain cycles in the range of 80 % in the case of the loose specimens and in the range of 35 % in the case of the dense specimens. The main part of this increase of stiffness took place during the first few hundred loading cycles.

Alarcon-Guzman et al. [4] used a testing device with integrated resonant column and torsional shear mode to study among other things the influence of a cyclic strain history on the shear modulus of dry coarse sand. They reported a moderate increase (approximately 5 %) of small strain shear modulus due to dynamic torsional prestraining with a large number of cycles with the amplitude $\gamma_{\text{prestrain}} = 1.3 \cdot 10^{-4}$ in the resonant column mode of the device. The authors stated that this increase reflects the reduction of void ratio due to prestraining. Thus, small strain shear modulus was said to be insensitive to cyclic strain history.

Lo Presti et al. [5] discussed the influence of dynamic prestraining on small strain shear modulus. Specimens were prestrained with 10,000 cycles of shear strain amplitudes between $\gamma_{\text{prestrain}} = 1.0 * 10^{-4}$ and $\gamma_{\text{prestrain}} = 8 * 10^{-4}$. After prestraining the small strain shear modulus of the specimens was measured and compared with the values of non-prestrained specimens. It was demonstrated that there was no increase of stiffness in the case of the specimens prestrained with amplitudes in the range of $\gamma_{\text{prestrain}} = 1.0 \cdot 10^{-4}$. The specimens prestrained with higher amplitudes showed only moderately higher values of G_0 in comparison with the non-prestrained specimens. Thus, it was concluded that dynamic prestraining with amplitudes lower than 10^{-3} has no significant influence on small strain shear modulus.

In a test series performed by Li et al. [6], [7], [8] specimens of fine sand were dynamically prestrained with an amplitude $\gamma_{\text{prestrain}}$ and after that the curves of shear modulus $G(\gamma)$ and damping ratio $D(\gamma)$ were determined over the whole range of achievable shear strain amplitudes. While the small strain shear modulus was somewhat increased due to prestraining the curve $G(\gamma)$ tended to converge to the curve of the non-prestrained specimens if γ approached the shear strain amplitude $\gamma_{\text{prestrain}}$. No significant difference could be observed in the curves of damping $D(\gamma)$ of non-prestrained and prestrained specimens in the range of amplitudes lower than $\gamma = 10^{-4}$. At higher shear strain amplitudes the values of damping ratio of the prestrained specimens were somewhat lower than the corresponding damping ratios of non-prestrained specimens. Around the prestraining amplitude $\gamma_{\text{prestrain}}$ a development of a plateau in the curves $G(\gamma)$ and $D(\gamma)$ was observed indicating that a signature of vibration history exists. At strains sufficiently higher than $\gamma_{\text{prestrain}}$ the curves of the non-prestrained and the prestrained specimens tended to coincide again. Li et al. stated that such a signature of vibration history could not be found in the case of previbration amplitudes lower than $\gamma_{\text{prestrain}} = 10^{-4}$ which is considered to be the elastic threshold strain. The signature of vibration history became more pronounced if the number of previbration cycles was increased. The density of specimens did not play an important role concerning the development of the plateaus. The plateaus developed in the curves of shear modulus were less significant than the signatures of vibration history in the curves of damping ratio versus strain γ.

A comprehensive study was performed by Tatsuoka et al. [9] in order to evaluate the influence of the method of sample preparation on shear modulus and damping properties of sand in drained resonant column and torsional shear tests. Specimens of a fine sand were reconstituded using different methods of preparation in order to produce different initial fabrics. Different methods of pouring (pluviating through air, pouring with a spoon) and compaction (vibration, tamping, tapping, rodding) were used. Specimens were prepared in the dry, moist or saturated condition. In some cases the water content was changed (i.e. decreased or increased) before the determination of shear modulus and damping ratio. Some other moist specimens were frozen for several weeks after preparation and saturated after thawing. From the test results Tatsuoka et al. concluded that shear modulus and damping ratio were insensitive to the method of sample preparation since the measured values of G and D did not differ significantly for specimens prepared by different meth-

ods. This was true for the small strain range but also for higher shear strain amplitudes. Thus, shear modulus and damping ratio were not affected by the initial fabric of the sand specimens.

3 Theoretical considerations

An increase of small strain stiffness due to cyclic strains can be expected from two reasons. The first possible cause of stiffness increase is the change of the shape of particle contacts. The modulus of elasticity E of a contact of two ideally round spheres of diameter D subjected to a vertical force F in the direction of the contact normal was derived by Hertz [10]:

$$E = \frac{3}{2}\left[\frac{2\bar{G}}{3(1-\bar{\nu})}\right]^{\frac{2}{3}} \sigma^{\frac{1}{3}} \quad (1)$$

with:

$\bar{G}$: shear modulus of sphere material
$\bar{\nu}$: Poisson's ratio of sphere material
σ: mean stress acting on the spheres $= F/D^2$

Goddard [11] derived the corresponding modulus of a contact of conus and sphere

$$E = \left(\frac{\bar{G}}{1-\bar{\nu}}\right)^{\frac{1}{2}} \left(\frac{6}{\pi\alpha}\right)^{\frac{1}{2}} \sigma^{\frac{1}{2}} \quad (2)$$

with α being the asperity angle of the conus. Goddard assumed equation (2) to be valid in the case of pressures σ below a transition pressure σ^* which can be deduced from equations (1) and (2):

$$\sigma^* = \frac{1}{96}\,\frac{\bar{G}}{1-\bar{\nu}}\,\pi^3\,\alpha^3 \quad (3)$$

If the contact pressure σ is increased above the value of σ^* equation (1) is valid. This assumption is shown schematically in Fig. 3 where F'-F represents the curve calculated from equation (1) and S'-S is the corresponding function received from equation (2). Goddard thought of Fig. 3 as a kind of "thermodynamic" phase diagram with the more stable phases being represented by the curve F'-F (contact sphere - sphere) and with the curve S'-S (contact conus - sphere) being a metastable phase below σ^* and non-existent for $\sigma > \sigma^*$. It has to be stated that the transition pressure σ^* is strongly dependent on the aspherity α of the contact conus - sphere. Goddard assumed that under prolonged vibration the relatively soft contacts of the type "conus - sphere" are replaced by stiffer and more stable hertzian contacts due to particle re-orientation and abrasion effects. The possible increase of stiffness due to a transition of the shape of particle contact is indicated by the vertical arrow in Fig. 3.

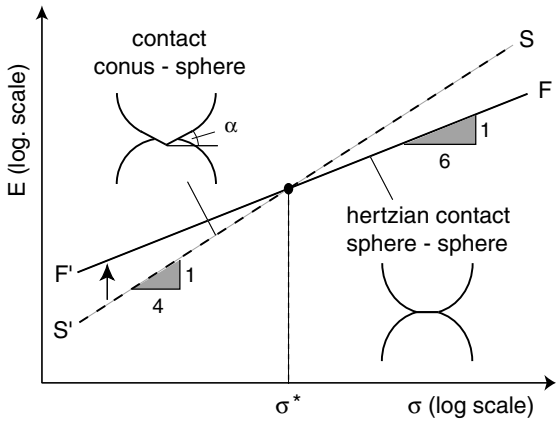

Fig. 3: Comparison of stiffnesses of contact types "sphere - sphere" and "conus - sphere" after Goddard

The second possible cause of an increase in sand stiffness due to an application of cyclic strains is the reduction of stress fluctuation. Consider the very simple example of an assembly of ideal round elastic spheres with hertzian contacts shown in Fig. 4a). The columns are only subjected to vertical forces. The external force F has to be distributed to the n columns of the sphere assembly in order to be conducted towards the bottom of the assembly. An uneven distribution of the force F to the particle columns is called stress fluctuation. If the force F is distributed evenly to $k < n$ columns one obtains the modulus of elasticity of the whole assembly from equation (4):

$$E^k = \frac{1}{c}\,k^{\frac{2}{3}} \quad (4)$$

with

$$c = \frac{3}{8}\left[\frac{8\bar{G}}{3(1-\bar{\nu})}\right]^{\frac{2}{3}} R^{-\frac{2}{3}} \quad (5)$$

R is the radius of the spheres. If this stiffness is compared with the modulus E^1 obtained in the case that only one column of spheres conducts the whole force F, one obtains the following relation:

$$\frac{E^k}{E^1} = k^{\frac{2}{3}} \quad (6)$$

A similar relationship can be deduced for the elastic (stored) energies W:

$$\frac{W^k}{W^1} = k^{-\frac{2}{3}} \quad (7)$$

If the contact law of the type "conus-sphere" is used one obtains the same equations as (6) and (7) but with an exponent 1/2 instead of 2/3. The curves resulting from (6) and (7) are presented in Figs. 4b) and 4c) for the case of an assembly of 100 identical columns of spheres.

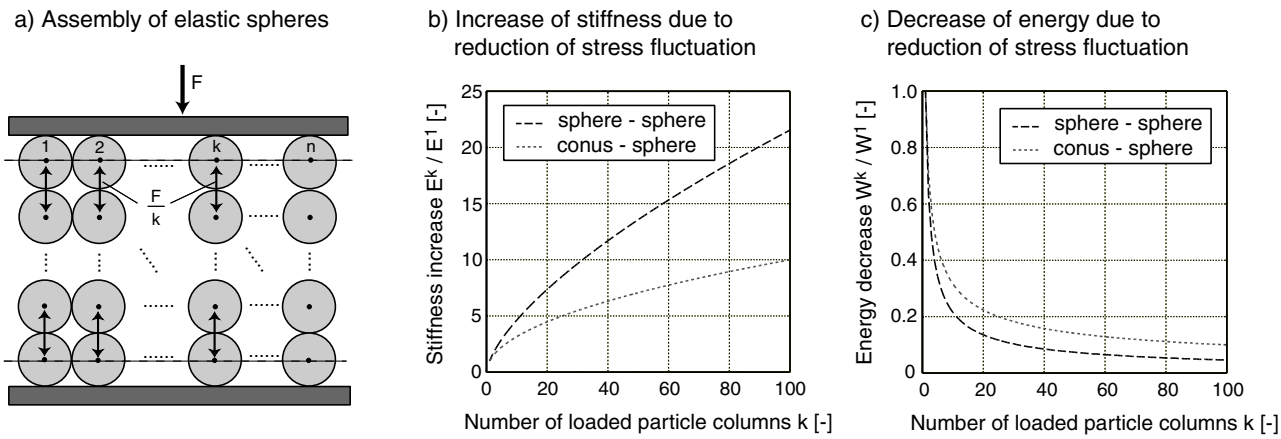

Fig. 4: *Stiffness increase and energy decrease due to reduction of stress fluctuation in an assembly of ideal spheres under consideration of different contact laws*

While the stiffness strongly increases when the boundary force is distributed more evenly the elastic energy of the particle assembly is reduced remarkable due to a reduction of stress fluctuation. Since the specimen tends to reach a condition of the lowest possible energy it can be expected that the application of cyclic strains leads to a soil fabric, whose stress fluctuation is smaller than that of a non-prestrained specimen. Thus, this would suggest that sand stiffness is increased due to cyclic strains.

A more detailed study of energies resulting from different stress fluctuations in particle assemblies using the "q-model" of Coppersmith [12] is given by Triantafyllidis and Niemunis [13].

4 Parameters affecting dynamic soil properties

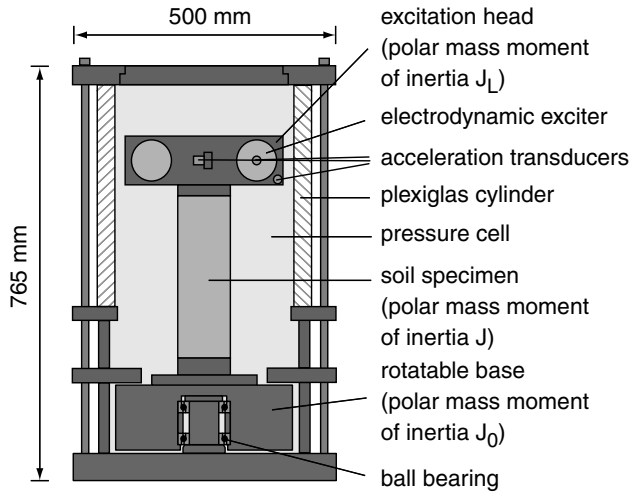

Fig. 5: Scheme of resonant column device used in this study

Fig. 5 shows a scheme of the resonant column (RC) device used in this study. The RC device belongs to the free - free type. The apparatus as well as the procedure of determination of shear modulus G, damping ratio D and shear strain amplitude γ as a mean value over the specimen volume is described in more detail in [14] and [15].

The tests documented in the present paper were performed on three different sands, one fine sand and two medium sands with nearly the same grain size distribution curve. The grain size distribution curves of the used sands are shown in Fig. 6. Table 1 summarizes the characteristic parameters of the distribution curves as well as the minimum and maximum densities for the respective materials. Specimens were prepared by pluviating dry sand out of a funnel through air into half-cylinder moulds. The distance between the sand surface and the funnel was kept konstant. Different combinations of fall height and funnel diameter resulted in different initial densities. Standard specimens with full cross section measured 10 cm in diameter and had a height of 30 cm. In the case of the hollow cylinder specimens an outer diameter of 10 cm, an inner diameter of 6 cm and a height of 10 cm was used in all tests.

Sand	ϱ_s	$\varrho_{d,\min}$	$\varrho_{d,\max}$	d_{50}	U
	$[\mathrm{g/cm^3}]$	$[\mathrm{g/cm^3}]$	$[\mathrm{g/cm^3}]$	[mm]	[-]
Fine sand	2.65	1.453	1.753	0.11	1.7
Medium sand 1	2.65	1.437	1.715	0.51	2.0
Medium sand 2	2.65	1.414	1.680	0.55	1.8

Table 1: Minimum / maximum densities and grain size characteristics of used sands ($U = d_{60}/d_{10}$)

The smallest resonant frequency in the tests on specimens with full cross section was $f_R \approx 24$ Hz in the case of low pressures ($p = 50$ kPa), medium

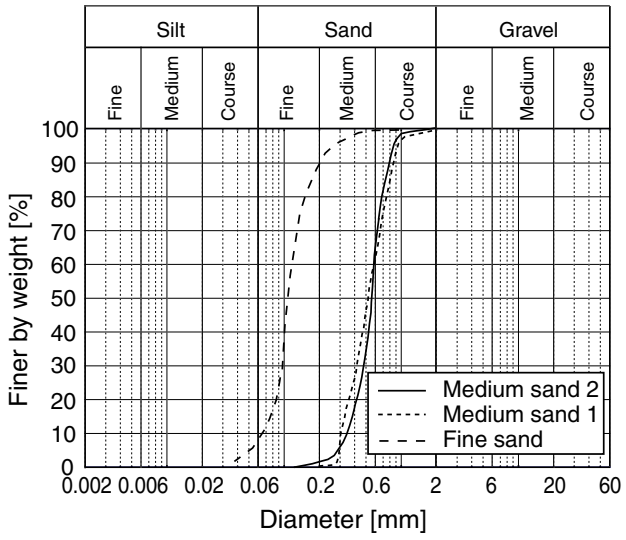

Fig. 6: Grain distribution curves of used sands

density ($I_D = 0.65$) and a shear strain amplitude of $\gamma = 3 \cdot 10^{-4}$. In the case of high pressures ($p = 800$ kPa) for dense sand ($I_D \approx 1.0$) and small shear strain amplitudes $\gamma \approx 10^{-6}$ the highest measured resonant frequency was $f_R \approx 66$ Hz. The resonant frequencies in the tests on hollow cylinder cross section specimens varied between $f_R \approx 40$ Hz ($p = 80$ kPa, $I_D = 0.45$, $\gamma \approx 9 \cdot 10^{-4}$) and $f_R \approx 70$ Hz ($p = 200$ kPa, $I_D = 0.65$, $\gamma \approx 10^{-6}$).

In order to obtain the dependence of small strain shear modulus G_0 on void ratio and confining pressure a test series was conducted. Full cylinder specimens of dry medium sand 2 (see Table 1) were prepared with different initial void ratios. A confining pressure of 50 kPa was first applied and the small strain shear modulus G_0 was measured. After that the confining pressure was raised and the value of G_0 was measured again. The confining pressure was increased towards 100, 200, 400 and 800 kPa in steps. In order to consider the aging effects described later a time period of two hours was waited between the raise of confining pressure and the measurement of small strain shear modulus within the respective pressure step. Since the volume changes due to the increase of confining pressure could not be measured in the RC device volume changes measured in parallel conducted test series in a triaxial cell with isotropic compression of the same sand were transferred to the series of RC tests [1].

Results of the twelve conducted tests are presented in Figs. 7a) and 7b). In Fig. 7a) the G_0 values versus void ratio at different confining pressures are presented. The volume changes during the increase of confining pressure have been taken into account within this diagram.

The well known decrease of G_0 with increasing void ratio at a constant confining pressure can be clearly observed. Fig. 7b) shows the dependence of small strain shear modulus on the confining pressure in a diagram using double logarithmic scale. Four tests with different initial void ratios e_0 and different initial relative densities $I_{D,0}$, respectively are shown in this diagram. As reported by previous investigators linear functions could be obtained using the chosen presentation. The following approximation of G_0 can be fitted:

$$G_0 = A \frac{(a-e)^2}{1+e} {p_a}^{1-n-m} {\sigma_a}^n {\sigma_p}^m \qquad (8)$$

with:

A:	factor, constant for a chosen soil
e:	void ratio
a:	constant factor representing a void ratio function
p_a:	atmospheric pressure
σ_a:	stress component in the direction of wave propagation
σ_p:	stress component in the direction of wave polarization
n, m:	exponents

Since the RC device used in the investigation is only capable to apply an isotropic state of stress ($p = \sigma_a = \sigma_p$) the often used assumption $n = m$ can be used and equation (8) can be simplified towards equation (9):

$$G_0 = A \frac{(a-e)^2}{1+e} {p_a}^{1-2n} p^{2n} \qquad (9)$$

From the adaption of the above formula to the experimental data the following parameters were received:

$$\begin{aligned} A &= 2.75 \\ a &= 1.46 \\ n &= 0.21 \end{aligned}$$

A comparison of the determined value of exponent n with data from the literature (e.g. Yu et al. [16] and Bellotti et al. [17]) leads to the conclusion that the value determined in the study described above lies in the lower range of measured exponents.

Furthermore the dependence of the small strain shear modulus on time was studied. Full cylinder specimens of dry medium sand 2 were built into the RC device and a confining pressure was applied and held constant. In definite time intervals the value of G_0 was determined. In the diagrams in Figs. 8a) and 8b) the measured small strain shear moduli G_0 at time t after the application of confining pressure are normalized with the values measured at time $t = 0$. Most of the tests were conducted over the time of at least

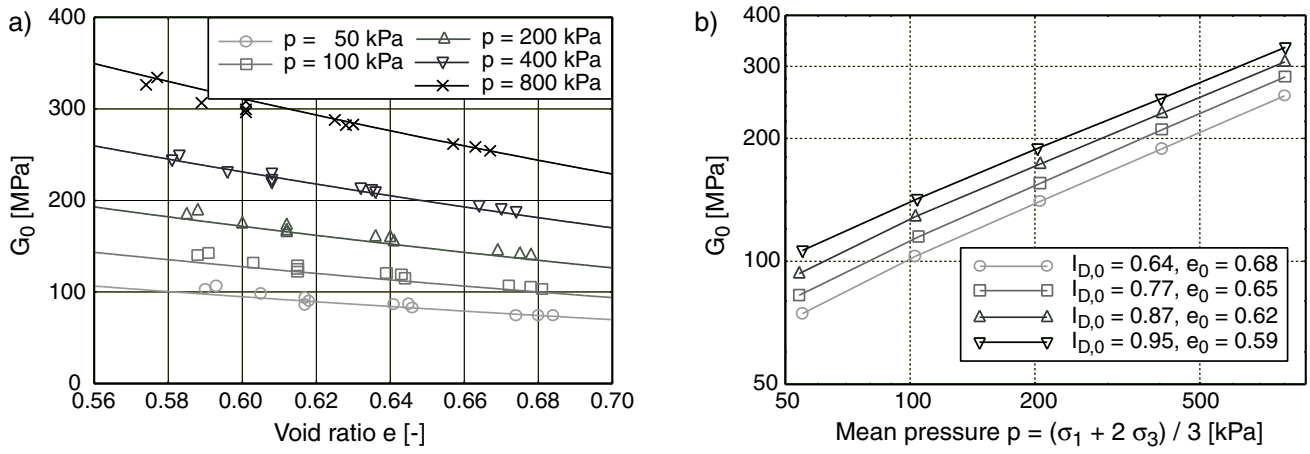

Fig. 7: *Dependence of small strain shear modulus on a) void ratio and b) confining pressure*

one week. Several initial densities and different confining pressures were tested. In Fig. 8a) tests with approximately the same density but different confining pressures are presented, while Fig. 8b) shows tests with identical confining pressure but different densities. A slight increase of small strain shear modulus with time could be determined in all tests. Nearly linear curves were received if the time axis is logarithmically scaled. As a measure of stiffness increase the slope N_G of the G_0 - ln(t) - curve is used in the literature. In all tests this slope seemed to increase especially after 1,000 minutes. These results coincide with observations made by Afifi and Woods [18] and Afifi and Richart [19] and also Baxter [20]. As Figs. 8a) and 8b) point out the stiffness increase lay between 4 and 6 % during the first 10,000 minutes under a constant confining pressure in all performed tests. From Fig. 8a) the conclusion can be drawn that a lower confining pressure results in a larger increase of small strain stiffness with time. Fig. 8b) shows that the increase of G_0 with time was not significantly affected by specimen density. These so called aging effects may be explained by micro-rearrangement of particle contacts and changes in the force fluctuations between the particles in order to accommodate the applied stress level. Time-rate effects at the contacts could be also a possible source for this behavior (see Di Benedetto et al. [21]).

Fig. 9 summarizes the influence of several parameters on the curves $G(\gamma)/G_0$ and $D(\gamma)$. Fig. 9a) and 9b) present the results of tests with hollow cylinder specimens of dry medium sand 2. Different relative densities were tested while the confining pressure was held constant at 80 kPa during this test series. No clear dependence of the curves $G(\gamma)/G_0$ and $D(\gamma)$ on void ratio could be determined. In the case of the curves of damping ratio it has to be stated that the values at small strains ($< 10^{-5}$) result from a quotient of two very small values and are thus less reliable than the values at higher strains. Figs. 9c) and 9d) compare $G(\gamma)/G_0$ and $D(\gamma)$ in the case of different confining pressures. The tests were conducted on full cylinder specimens of dry medium sand 2. The relative density was held approximately constant during this test series. It can be concluded that the shear modulus degraded faster in the case of a lower confining pressure whilst a faster increase of damping ratio with increasing shear strain amplitude was measured at lower confining pressures. Figs. 9e) and 9f) summarize tests conducted on full and hollow cylinder specimens in order to compare the influence of the two specimen geometries on the curves $G(\gamma)/G_0$ and $D(\gamma)$. Specimens were prepared with nearly identical initial density and a confining pressure of 200 kPa was chosen. It can be stated that the full cylinder specimens tended to a slightly faster reduction of shear modulus with increasing shear strain amplitude than the specimens with hollow cross section. With the exception of the range of small shear strain amplitudes the curves of damping ratio of full and hollow cylinder specimens agreed well.

5 Change of dynamic properties of specimens with full cross section due to dynamic prestraining in the resonant column device

In additional test series dynamic torsional prestraining was applied to the specimens in the RC device. After the application of confining pressure in the RC device the shear strain amplitude γ was increased up to a value $\gamma_{\mathrm{prestrain}}$. The values of shear modulus $G(\gamma)$ and damping ratio $D(\gamma)$ were measured with increasing shear strain amplitude and correspond to the properties of the non-prestrained specimen. When the shear strain amplitude $\gamma_{\mathrm{prestrain}}$ was reached, it was held constant and the specimen was subjected to a definite number of cycles $N_{\max}$ with $\gamma_{\mathrm{prestrain}}$ being the amplitude. After a definite number of strain cycles $N < N_{\max}$ the shear

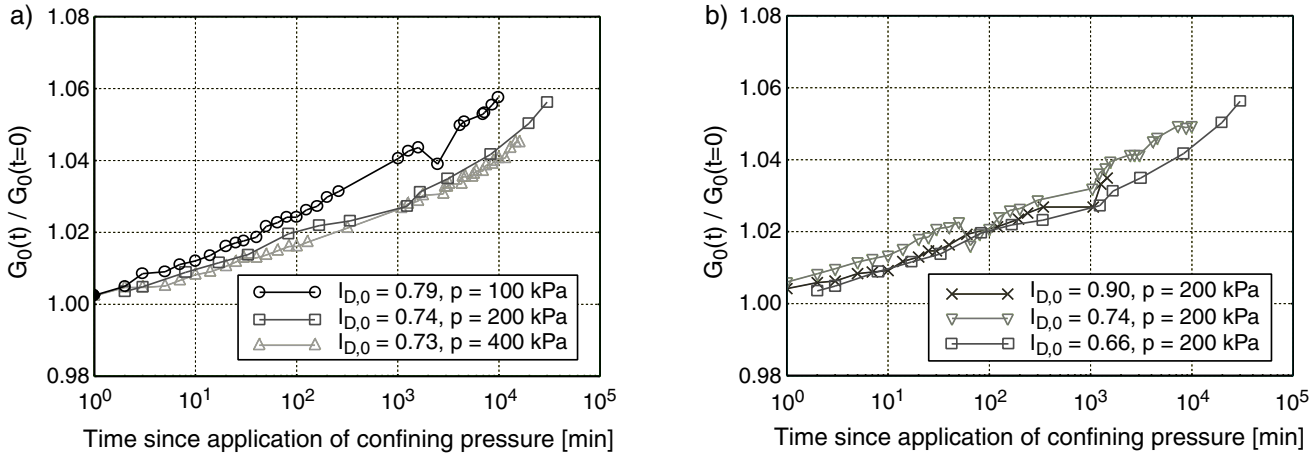

Fig. 8: *Dependence of small strain shear modulus on time: a) influence of confining pressure, b) influence of density*

strain amplitude was reduced to $\gamma \approx 10^{-6}$ in order to observe possible changes in the shear modulus at small strains G_0 caused by the prestraining. Thereafter the strain amplitude was increased again to the value of $\gamma_{\text{prestrain}}$. During this decrease and re-increase of shear strain amplitude the values of shear modulus $G(\gamma)$ and damping ratio $D(\gamma)$ were measured. Thus, changes in the values of shear modulus and damping ratio in the range of shear strain amplitudes between $\gamma = 10^{-6}$ and $\gamma_{\text{prestrain}}$ could be detected. Having reached the prestraining amplitude $\gamma_{\text{prestrain}}$ further cycles were performed. This procedure was repeated several times during the dynamic prestraining at different strain cycles $N < N_{\max}$. In the latest stage of the test the shear strain amplitude was increased towards the maximum applicable value $\gamma_{\max}$ passing the prestraining amplitude $\gamma_{\text{prestrain}}$.

Figs. 10a) and 10b) show the resulting curves of shear modulus G and damping ratio D versus the shear strain amplitude γ for a representative test. The test in these Figs. was carried out with a full cylinder specimen of fine sand and a confining pressure of $p = 200$ kPa. The specimen was prepared with a relative density of $I_{D,0} = 0.64$ and was subjected to a prestraining with totally $N_{\max} = 3 \cdot 10^6$ cycles and an amplitude of $\gamma_{\text{prestrain}} = 10^{-4}$. From Figs. 10a) and 10b) one can see, that plateaus have been developed in the curves $G(\gamma)$ and $D(\gamma)$ as a result of torsional prestraining at the location of the prestraining amplitude $\gamma_{\text{prestrain}}$. This material behaviour was already observed by Li et al. [6], [7], [8]. The shear modulus at small strains G_0 after the first reduction of shear strain amplitude did not reach the original value of the non-prestrained specimen and it was slightly lower. During the dynamic torsional prestraining the shear moduli G_0 and G($\gamma_{\text{prestrain}}$) stayed almost constant. At shear strains sufficiently higher than $\gamma_{\text{prestrain}}$ the curves of shear modulus and damping ratio tended to approach the curves of the non-prestrained specimens again.

The dependence of the plateau size on the number of applied cycles $N_{\max}$ and the shear strain amplitude during prestraining $\gamma_{\text{prestrain}}$ was studied on full cylinder specimens. The relative density of $I_{D,0} \approx 0.65$ and the confining pressure of $p = 200$ kPa were held constant during the test series. The sand (fine sand as well as medium sand 1 were studied) and the shear strain amplitude during prestraining ($\gamma_{\text{prestrain}} = 0.5 \cdot 10^{-4}$ and $\gamma_{\text{prestrain}} = 1.0 \cdot 10^{-4}$) were variied. The results of shear modulus and damping ratio from the experiments on fine sand with a prestraining amplitude $\gamma_{\text{prestrain}} = 1.0 \cdot 10^{-4}$ are documented in Figs. 11 and 12, respectively where different $N_{\max}$ (maximum number of cycles) have been applied. The shear modulus G is divided through the shear modulus at small strains $G_0(N = 0)$ measured before prestraining and the damping ratio D is also normalized with the value of the non-preloaded specimen at small strains. From Figs. 11 and 12 it can be clearly seen that the size of the plateaus increased with increasing number of cycles. The sand memorizes not only the magnitude of the shear strain amplitude during prestraining $\gamma_{\text{prestrain}}$ but also the number of applied strain cycles which can be estimated from the size of the plateau area. The plateaus in the curves of damping ratio were more pronounced than the plateaus in the respective curves of shear modulus.

In order to quantify the size of the plateaus a plateau area was defined. The start and end points of the plateau area are chosen as presented in Figs. 13a) and 13b). The plateau area in the curve of the normalized shear modulus is determined as follows. As the starting point for the plateau the turning point of the curve $G(\gamma)$ during the last re-increase of shear strain amplitude after the application of the maximum number of cycles is chosen. From this point the curve $G(\gamma)$ flat-

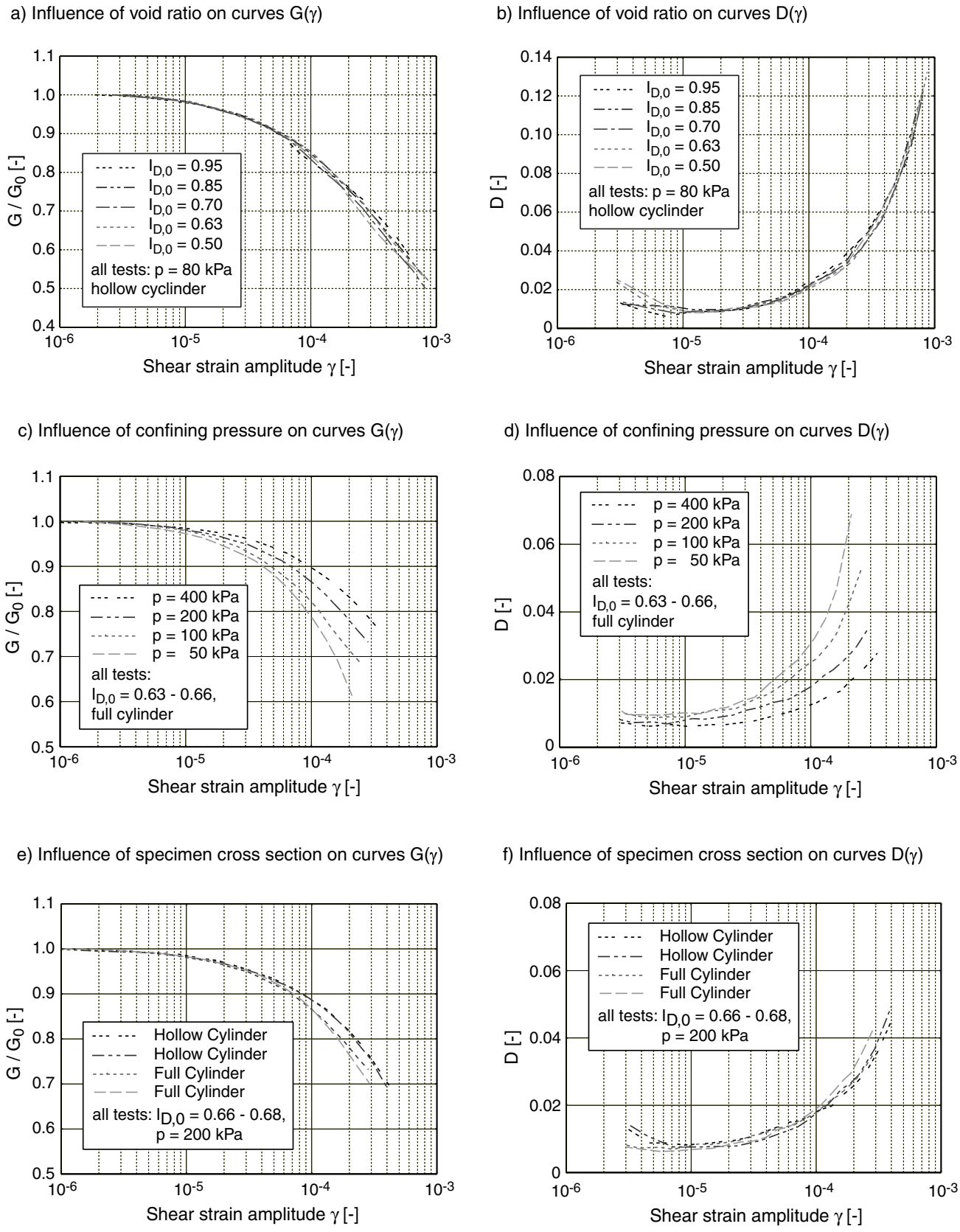

Fig. 9: *Dependence of curves of shear modulus $G(\gamma)$ and damping ratio $D(\gamma)$ on void ratio, confining pressure and specimen geometry*

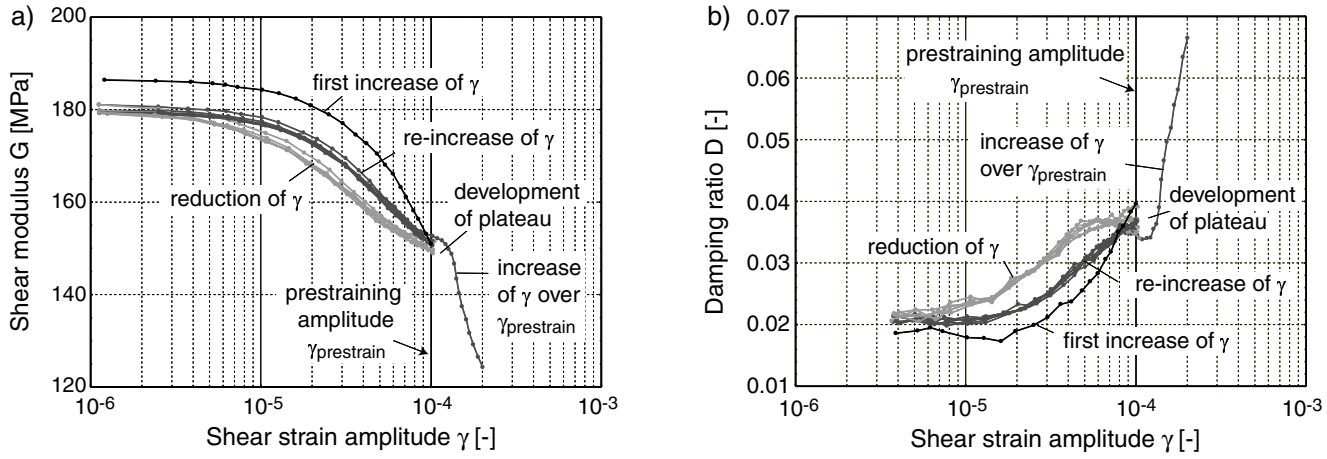

Fig. 10: *Development of plateaus in the curves a) $G(\gamma)$ and b) $D(\gamma)$ due to dynamic prestraining in the RC device, test on dry fine sand with $N_{\max} = 3 \cdot 10^6$ cycles, confining pressure $p = 200$ kPa and initial relative density $I_{D,0} = 0.64$*

tens. The end point of the plateau area is defined as the point of the curve $G(\gamma)$ after the shear strain amplitude γ was increased to values higher than $\gamma_{\text{prestrain}}$ at which the slope of the curve is equal again to the slope of the curve $G(\gamma)$ of the non-prestrained specimens. The area between the linear connection of start and end point and the curve $G(\gamma)$ is called $A_{P,G}$. Analogously the plateau area in the curve of the damping ratio is determined. This area is named $A_{P,D}$.

Fig. 14a) shows the calculation results of the plateau areas as obtained from the curves of the normalized shear modulus. Four series of tests were carried out. Two values of $\gamma_{\text{prestrain}}$ and different $N_{\max}$ values were tested for each sand. For all combinations of sand, $\gamma_{\text{prestrain}}$ and $N_{\max}$ two tests were performed. The average values of the plateau areas of each test series with a definite sand and a constant $\gamma_{\text{prestrain}}$ are connected linearly in order to simplify the comparison between the curves. The enlargement of the plateaus with increasing number of cycles can be clearly seen. If the applied number of cycles was identical but the shear strain amplitude during prestraining was different the signature of vibration history was more significant in the case of the higher prestraining amplitude. In this test series the plateau area in the curves of shear modulus was approximately doubled when the shear strain amplitude during prestraining $\gamma_{\text{prestrain}}$ was doubled from $0.5 \cdot 10^{-4}$ to $1.0 \cdot 10^{-4}$. There were hardly any differences concerning the development of the plateaus between fine and medium sand. Nearly the same conclusions could be drawn from the analysis of the plateau areas in the curves of damping ratio, which are presented in Fig. 14b). However, the curve representing the results for medium sand with $\gamma_{\text{prestrain}} = 1.0 \cdot 10^{-4}$ lay at significantly lower values compared to the curve of the fine sand under the same loading conditions. Some of the data points even lay in the range of the curves with $\gamma_{\text{prestrain}} = 0.5 \cdot 10^{-4}$. This may indicate that for evaluation purposes the results from the damping ratio plateau may be more pronounced with respect to the material under investigation. The determined plateau areas in the curves of shear modulus and damping ratio showed a visible scattering around the mean values. In comparison with the results of Li it has to be stated that a visible signature of vibration history could be determined even in the case of shear strain amplitudes below the elastic threshold strain $\gamma = 10^{-4}$ because the development of plateaus was also observed in the tests with a prestraining amplitude of $\gamma_{\text{prestrain}} = 0.5 \cdot 10^{-4}$.

The change of small strain shear modulus G_0 due to prestraining with a large number of strain cycles is shown in Fig. 15 for the four test series. It can be stated that the reduction of small strain shear modulus due to the first 10,000 strain cycles was larger in the case of the medium sand than for fine sand and it was even larger for the higher prestraining amplitudes. This reduction did not exceed a value of 7 % for the performed tests. After this reduction due to the first strain cycles the small strain shear modulus only slightly increased with increasing number of applied strain cycles. This increase of G_0 was slightly larger for the larger prestraining amplitude. In the case of the fine sand a slightly larger increase was observed in comparison with the medium sand. However this increase did not exceed 10 % during 10 million cycles with shear strain amplitudes $\gamma_{\text{prestrain}} = 1.0 \cdot 10^{-4}$.

The development of the signature of prestraining history may be more pronounced when packages of cycles with different shear strain amplitudes $\gamma_{\text{prestrain}}$ are applied in succession. In a test at first 3 million cycles with $\gamma_{\text{prestrain},1} = 0.5 \cdot 10^{-4}$ were applied followed by

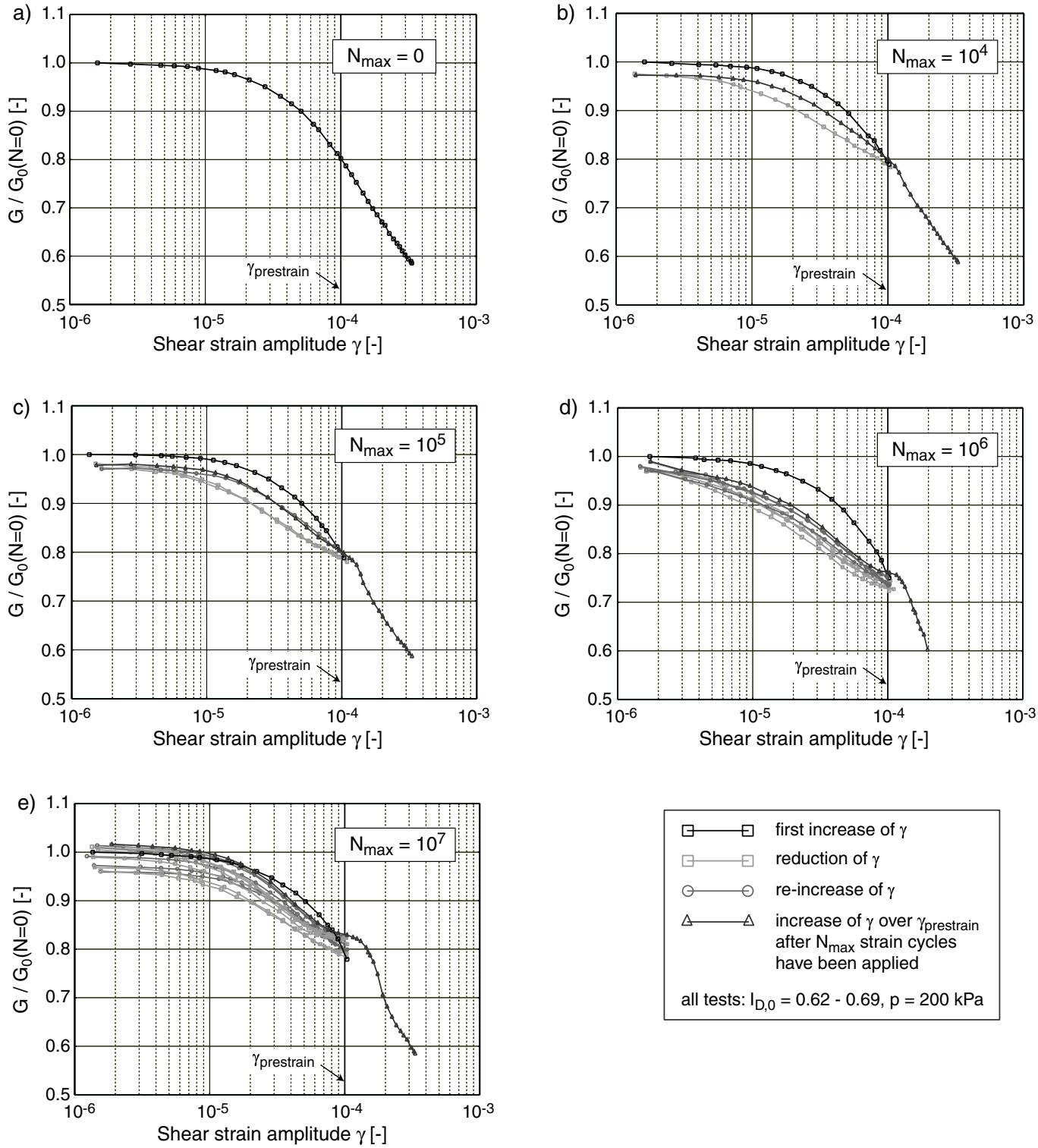

Fig. 11: *Development of plateaus in the curves $G(\gamma)$ with increasing number of applied strain cycles, tests on dry fine sand*

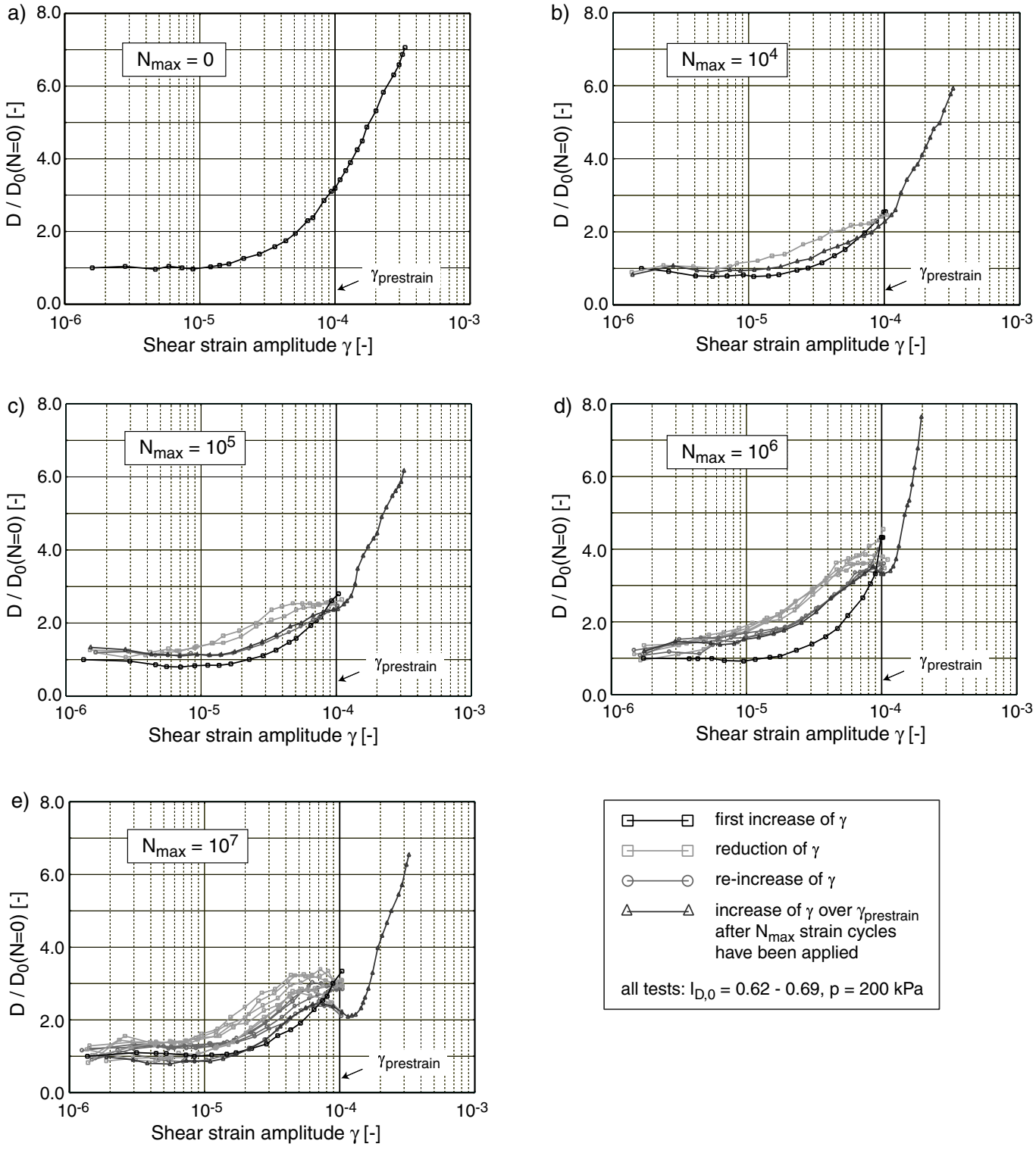

Fig. 12: *Development of plateaus in the curves $D(\gamma)$ with increasing number of applied strain cycles, tests on dry fine sand*

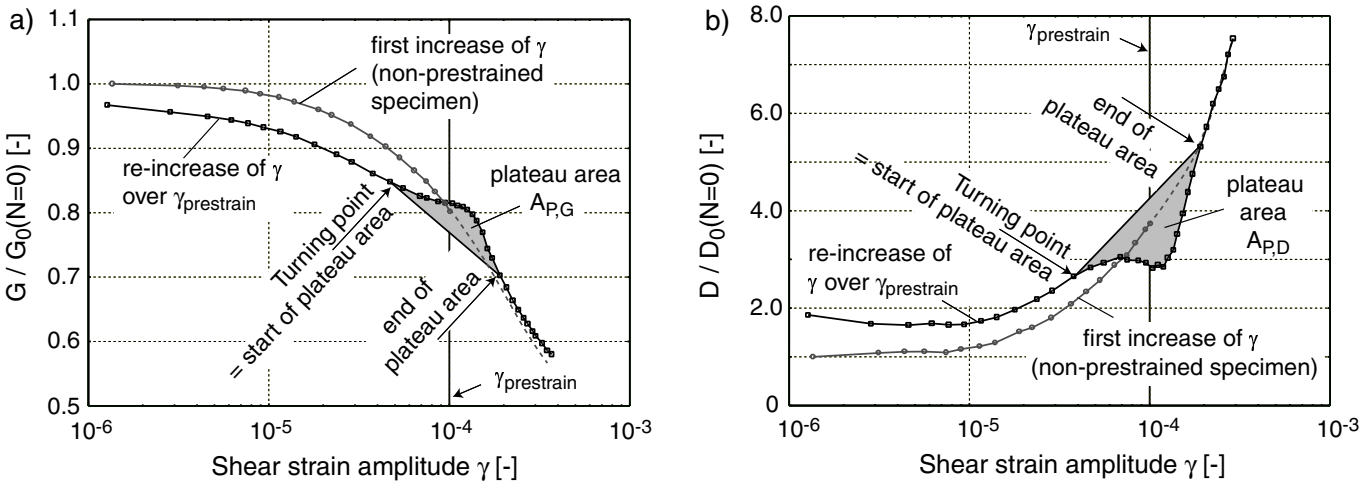

Fig. 13: *Definition of plateau areas a) $A_{P,G}$ in the curve $G(\gamma)$ and b) $A_{P,D}$ in the curve $D(\gamma)$*

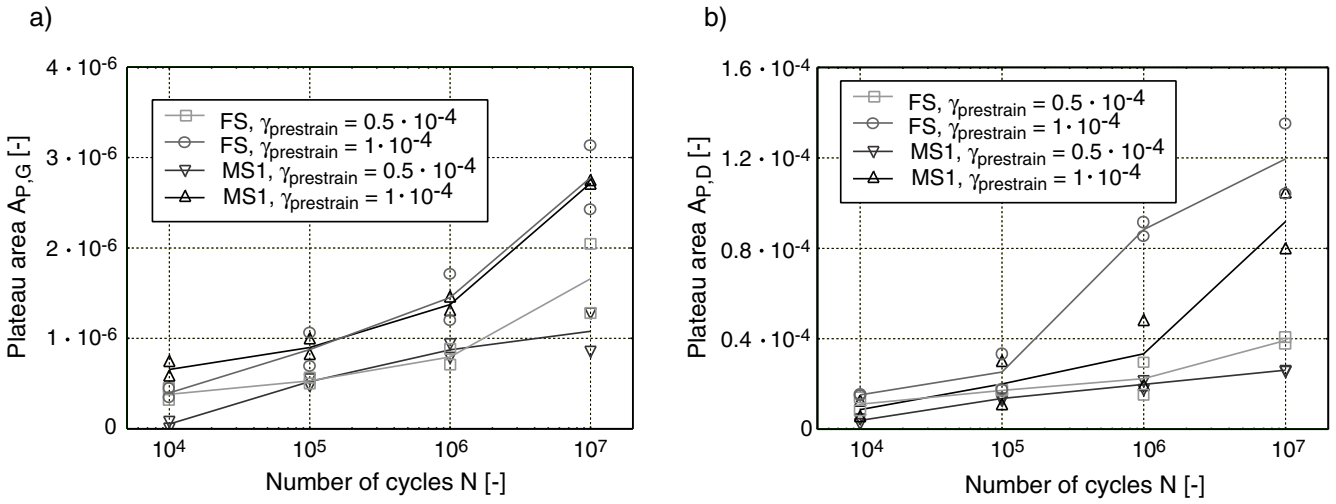

Fig. 14: *Plateau areas a) $A_{P,G}$ and b) $A_{P,D}$ as a function of the number of cycles, the prestraining amplitude and the sand (FS: fine sand, MS1: medium sand 1)*

3 million cycles with $\gamma_{\text{prestrain},2} = 1.0 \cdot 10^{-4}$ and finally the specimen was subjected to 3 million cycles with a shear strain amplitude of $\gamma_{\text{prestrain},3} = 2.0 \cdot 10^{-4}$. The resulting curves of shear modulus and damping ratio are shown in Figs. 16a) and 16b). It can be seen that when the prestraining amplitude $\gamma_{\text{prestrain}}$ was increased in succeeding packages the sand always memorized the last value of $\gamma_{\text{prestrain}}$ and forgot the preceeding prestraining amplitudes. If the prestraining amplitude e.g. was increased from $\gamma_{\text{prestrain},1} = 0.5 \cdot 10^{-4}$ to $\gamma_{\text{prestrain},2} = 1.0 \cdot 10^{-4}$ one could observe a plateau around $\gamma_{\text{prestrain},1} = 0.5 \cdot 10^{-4}$. This plateau was not visible any more when the shear strain amplitude was reduced to zero and then increased again to $\gamma_{\text{prestrain},2} = 1.0 \cdot 10^{-4}$. With increasing number of cycles applied with the new value of $\gamma_{\text{prestrain}}$ a new plateau was developed around this prestraining amplitude. Another material behavior could be observed when at first a package of cycles with an amplitude $\gamma_{\text{prestrain},1} = 1.0 \cdot 10^{-4}$ was applied to the specimen followed by a package with cycles at a lower amplitude $\gamma_{\text{prestrain},2} = 0.5 \cdot 10^{-4}$. Figs. 16c) and 16d) contain the results of such a test. After the application of three million strain cycles with each of these prestraining amplitudes the shear strain amplitude was decreased to zero and finally increased to the possible maximum value of γ passing the two values of prestraining amplitude $\gamma_{\text{prestrain}}$. In this case a curve was observed that enveloped both plateaus obtained if only one package of cycles with $\gamma_{\text{prestrain}} = 1.0 \cdot 10^{-4}$ or $\gamma_{\text{prestrain}} = 0.5 \cdot 10^{-4}$ would have been applied. This envelope was observed for both curves $G(\gamma)$ and $D(\gamma)$. Thus, the sequence of applied packages of cycles seems to play an important role for densification processes. Applying first the cy-

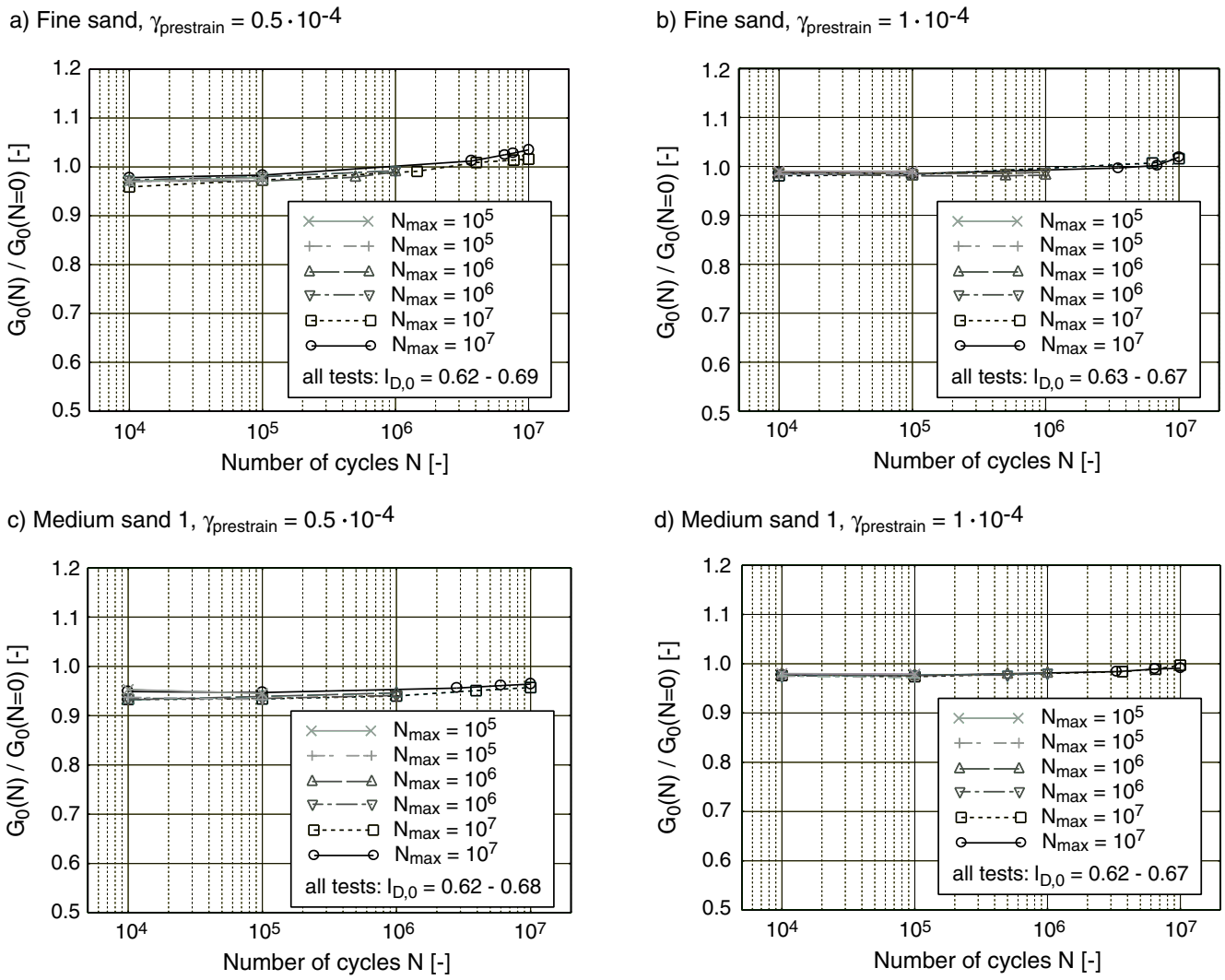

Fig. 15: *Developement of small strain shear modulus during dynamic torsional prestraining*

cles of the highest strains and subsequently the cycles of the lowest strains leads to a stiffer material behaviour within the limits of the prestraining amplitudes and at the same time also to smaller material damping in comparison to the reverse procedure. This knowledge may be used for construction processes.

Furthermore the influence of a change in the state of stress after prestraining on the signature of strain history was examined. A full cylinder specimen was prestrained with 3.5 million cycles with an amplitude $\gamma_{\mathrm{prestrain}} = 1.0 \cdot 10^{-4}$ at a confining pressure of p = 200 kPa. After prestraining the confining pressure was increased to $p = 225$ kPa in one test and reduced to $p = 175$ kPa in another test. Figs. 17a) and 17b) show the curves $G(\gamma)/G_0$ and $D(\gamma)$ after the increase of confining pressure and in Figs. 17c) and 17d) the result of the reduction of confining pressure is presented. It can be concluded that the shear strain amplitude during prestraining $\gamma_{\mathrm{prestrain}}$ could still be localized from the curves $G(\gamma)$ and $D(\gamma)$, the magnitude of the plateau however had decreased in comparison with a test in which the confining pressure during prestraining and the succeeding measurement of the curves $G(\gamma)$ and $D(\gamma)$ was held constant. A change of stress level seems to destroy the signs of vibration history and this destruction seems to increase with increasing stress changes.

6 Change of dynamic properties of hollow cylinder specimens due to dynamic prestraining in the resonant column device

In another test series the influence of the homogeneity of the shear strain distribution over the specimen cross section was studied. Hollow cylinder specimens with the geometry described in chapter 4 were subjected to a dynamic prestraining in the resonant column device. Different prestraining amplitudes $\gamma_{\mathrm{prestrain}}$ were tested

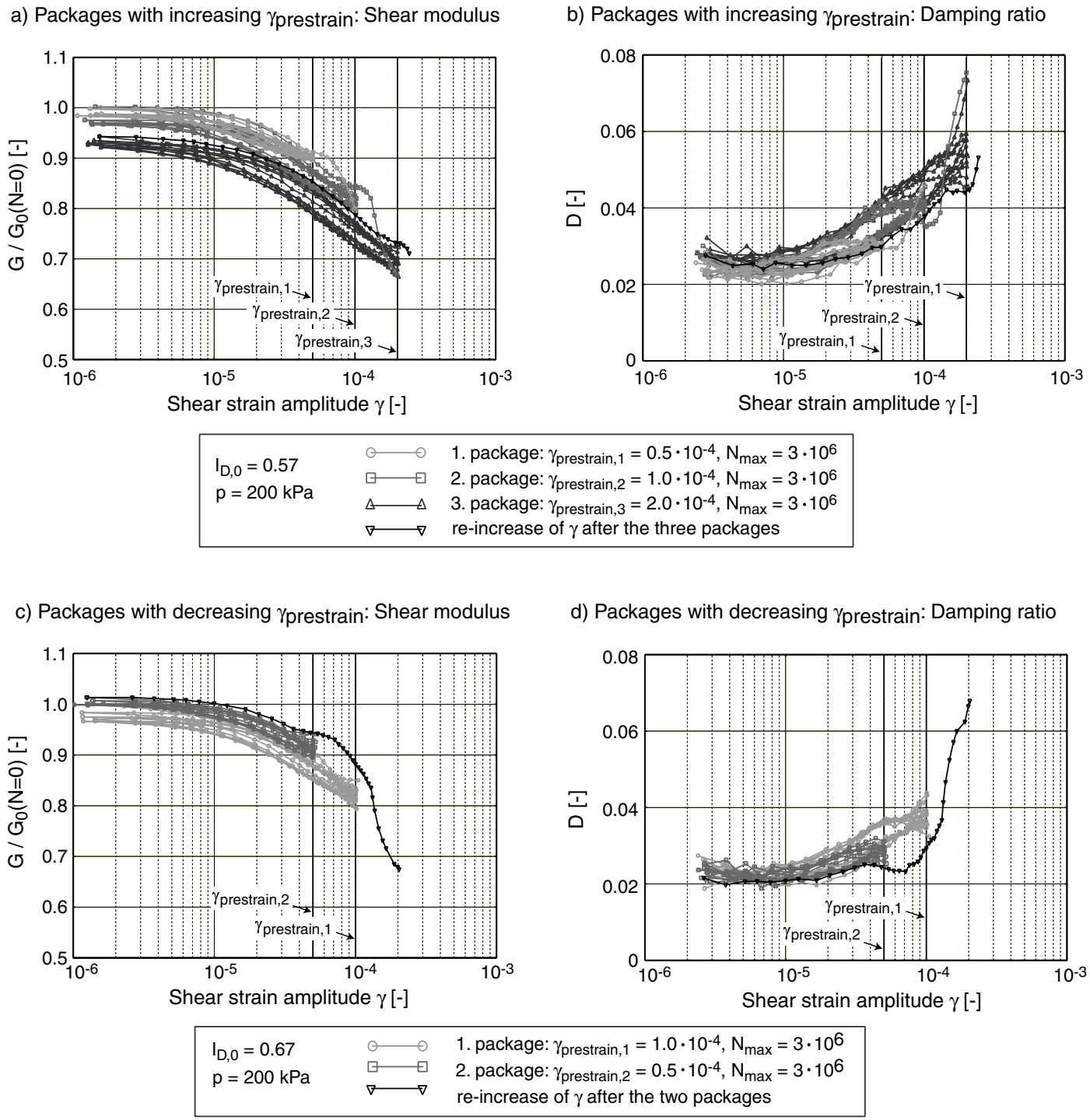

Fig. 16: *Developement of signatures of strain history in the case of a subsequent application of packages of cycles with different prestraining amplitudes, tests on dry fine sand*

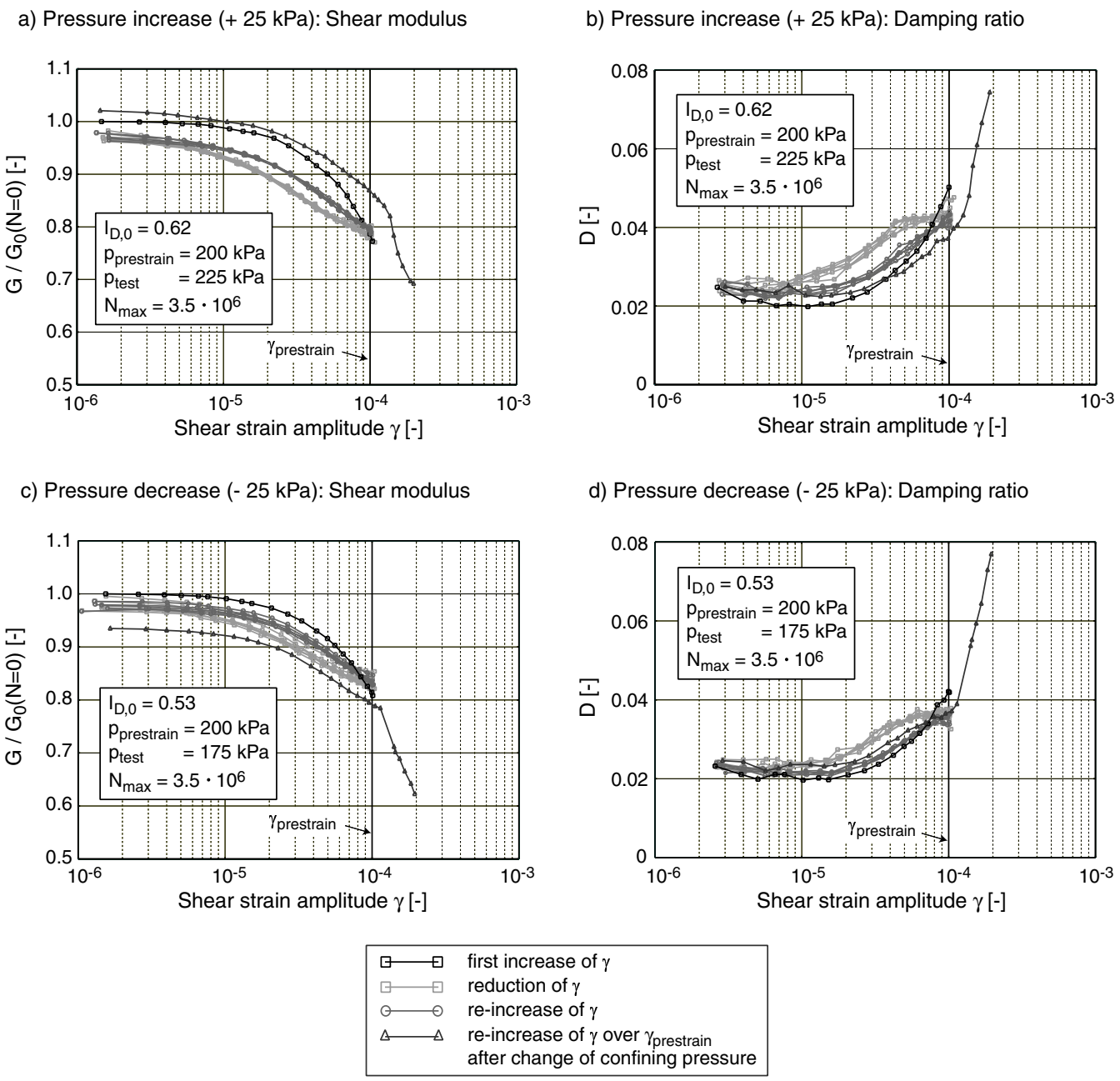

Fig. 17: *Influence of a change of confining pressure after prestraining on the signatures of strain history, tests on dry fine sand*

on specimens of fine sand and medium sand 2, respectively. The initial relative densities of the specimens for all tests were within the range of 0.63 and 0.70. Confining pressure was chosen as 200 kPa and five million strain cycles were applied in all tests. Similar to the full cylinder specimens the shear strain amplitude was reduced and re-increased after certain numbers of applied strain cycles in order to measure the small strain shear modulus G_0. Fig. 18a) presents the development of small strain shear modulus with the number of applied cycles in the case of specimens of fine sand and prestraining amplitudes between $\gamma_{\mathrm{prestrain}} = 0.5 \cdot 10^{-4}$ and $\gamma_{\mathrm{prestrain}} = 2.0 \cdot 10^{-4}$. In all tests a small increase of G_0 with increasing number of cycles independent on prestraining amplitude was measured. This observation coincides well with the tests on full cylinder specimens presented in Figs. 15a) and 15b).

Fig. 18b) shows the development of G_0 versus the number of applied strain cycles in the case of the tests on hollow cylinder specimens of medium sand 2. In contradiction to the test results of fine sand a slight decrease of G_0 during the first one million cycles can be

observed. This decay was more significant in the case of higher prestraining amplitudes. Between one million and five million applied load cycles stagnation or a small re-increase of G_0 could be determined. In similar tests on full cylinder specimens presented in Figs. 15c) and 15d) a small continuous increase of small strain shear modulus was determined between 10,000 and ten millions applied strain cycles. However, only small prestraining amplitudes were tested in the series with full cylinder specimens and those tests were conducted with the medium sand 1. From Fig. 18b) it can be concluded, that the decrease of small strain shear modulus due to the first 10,000 strain cycles was becoming more pronounced when a higher prestraining amplitude was chosen. This can also be seen in Fig. 18d) where the measured curves of shear modulus $G(\gamma)$ normalized with G_0 during the first increase of shear strain amplitude up to $\gamma_{\text{prestrain}}$ and the succeeding decrease after 10,000 applied strain cycles are presented. As can be seen from Figs. 18a) and 18c) in the tests on fine sand small strain shear modulus after 10,000 applied strain cycles reached the value of the non-prestrained specimens $G_0(N = 0)$ independently of the applied prestraining amplitude.

In the tests conducted with hollow cylinder specimens a signature of prestraining in the curves $G(\gamma)$ and $D(\gamma)$ at prestraining amplitude $\gamma_{\text{prestrain}}$ could also be observed. The plateaus were more significant in the case of the fine sand than for medium sand 2. From the comparison of the tests with dynamic prestraining of full and hollow cylinder specimens in the RC device it can be concluded that the distribution of shear strains over the specimen cross section seems not to play an important role concerning the material behaviour under cyclic or dynamic torsional prestraining. Similar small changes of G_0 were determined in the case of both geometries of specimen's cross section.

7 Change of dynamic properties due to cyclic prestraining with high shear strain amplitudes

Another test series was performed in order to study if higher shear strains during cyclic prestraining result in a more significant change of small strain material properties since the prestraining amplitudes that could be applied to specimens in the RC device did not have a large effect on small strain shear modulus. In order to apply higher shear strains to hollow cylinder specimens the simple device (which is further named torsional shear device) shown schematically in Fig. 19 was designed and constructed. An electric motor is equipped with an excenter whose rotation is transferred towards a sinusoidal horizontal motion of a cantilever. The cantilever is mounted with a load piston which is vertically conducted by means of a ball bearing. The load piston is fixed with the top end plate of the hollow cylinder specimen. Thus, a sinusoidal twisting of the load piston is transferred as shear strain to the specimen. The use of different excenters results in the subjection of different shear strain amplitudes.

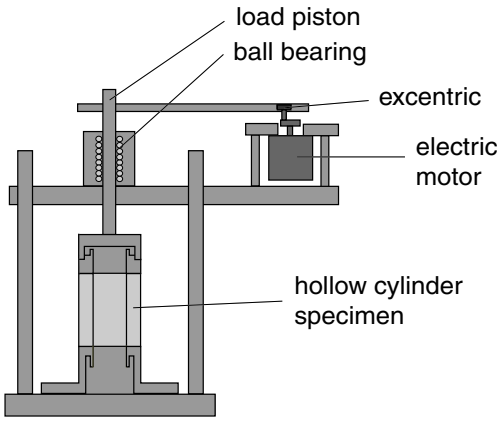

Fig. 19: Scheme of torsional shear device

Specimens were prepared outside this device by the pluviating method and a vacuum of 80 kPa was applied to the grain skeleton. The geometry of the specimens was measured. Then specimens were transported towards the torsional shear device and the load piston was fixed with the top end plate of the specimens. The desired number of strain cycles with the specified shear strain amplitude was applied. After this prestraining the geometry of the specimen was measured once again in order to calculate the change of void ratio due to prestraining. Specimens were transported from the torsional shear device towards the resonant column device and built into this apparatus. The vacuum was reduced in small steps of 10 kPa and the confining pressure was increased simultaneously in the same steps until a confining pressure of 80 kPa was reached and the vacuum was equal zero. Thus, the effective pressure was held constant during prestraining and the succeeding measurement of dynamic soil properties within the RC apparatus. Medium sand 2 was used in all these tests and specimens were prestrained with a frequency of 0.6 Hz in the torsional shear device. The applied prestraining amplitudes were chosen as $\gamma_{\text{prestrain}} = 5 \cdot 10^{-3}$ and $\gamma_{\text{prestrain}} = 10^{-2}$ with $N_{\max} = 100$, 1,000, 10,000 or 50,000 strain cycles. At least four tests with specimens of different initial densities were performed with identical maximum number of cycles and identical prestraining amplitude.

For comparison purposes tests on non-prestrained specimens of different initial densities have been carried out in the RC device. The confining pressure was chosen as $p = 80$ kPa in all these tests. The small strain shear moduli G_0 observed in these tests are presented

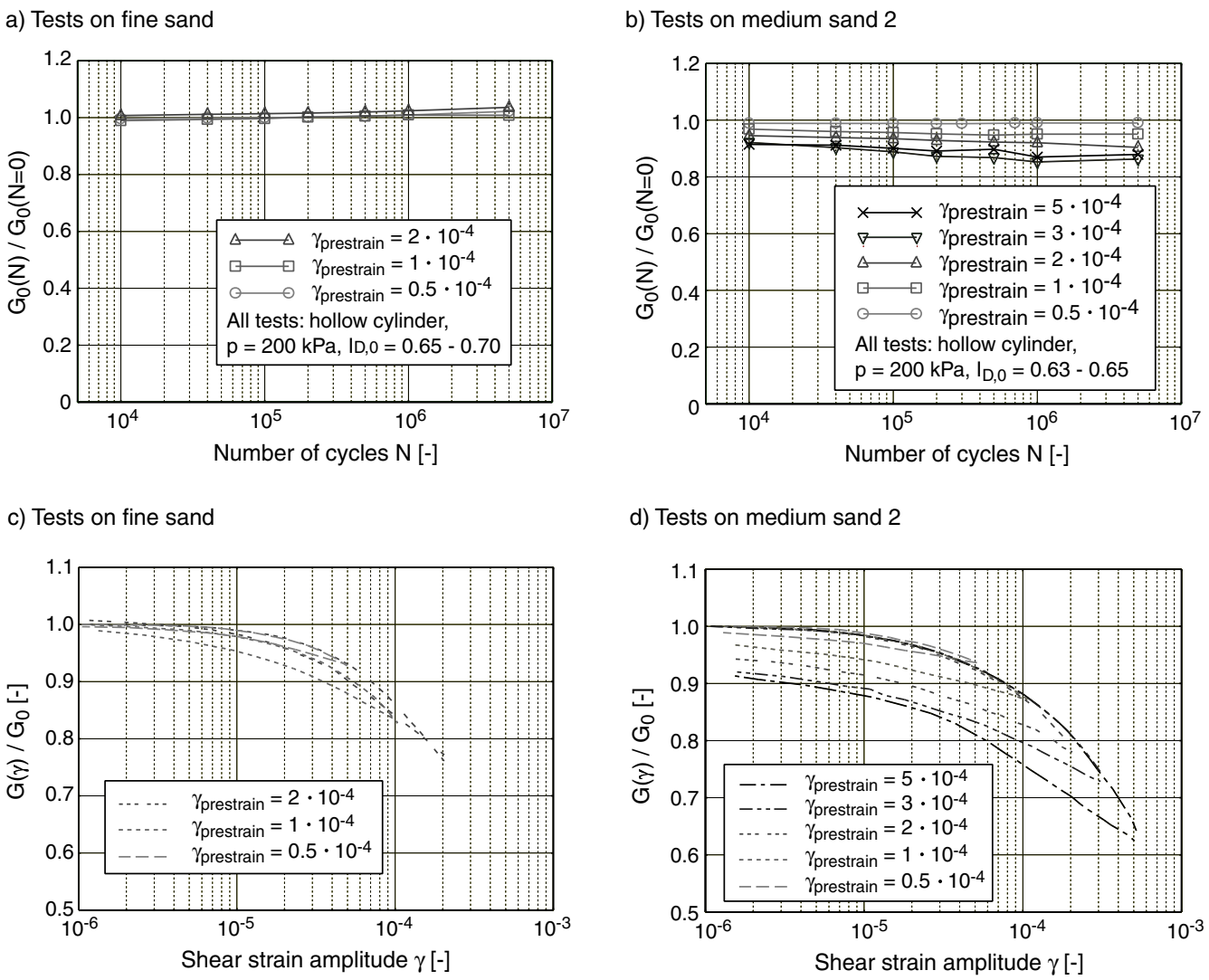

Fig. 18: *Developement of small strain shear modulus G_0 during dynamic torsional prestraining of hollow cylinder specimens (a,b) and the corresponding curves $G(\gamma)/G_0$ during the first increase of γ towards $\gamma_{prestrain}$ and during the succeeding decrease of γ after 10,000 applied cycles (c,d)*

as gray filled circles in Figs. 20a) and 21a) and could be approximated by the function

$$G_0(p = 80 \text{ kPa}) \quad = \quad 113 \text{ MPa } \frac{(1.88 - e)^2}{1 + e} \quad (10)$$

The shear moduli calculated from (10) are shown as gray solid line in Figs. 20a) and 21a). It has to be stated that all the measured curves of $G(\gamma)/G_0$ and $D(\gamma)$ of the non-prestrained specimens lay within a narrow band indepentent of the void ratio of the specimens.

Fig. 20a) compares the measured small strain shear moduli G_0 of specimens prestrained with $\gamma_{\text{prestrain}} = 5 \cdot 10^{-3}$ with the values determined from the tests on non-prestrained specimens. The values of G_0 are presented as a function of void ratio after prestraining. The test data in Fig. 20a) indicates that small strain shear moduli of specimens prestrained with 100 cycles lay slightly below the curve of the mean values of non-prestrained specimens. The higher the number of applied cycles was the higher were the measured values of small strain shear moduli in comparison with the non-prestrained specimens of identical void ratio. All the values of the specimens prestrained with 50,000 cycles could be found above the mean curve of the non-prestrained specimens.

In Fig. 20c) the measured values of G_0 of the prestrained specimens were normalized with shear moduli calculated from (10). The void ratio after prestraining was used for this purpose. The normalized small strain shear modulus after prestraining is presented as a function of the number of applied strain cycles. Mean values of the data points with identical number of cycles were

a) $G_0(e)$ of prestrained and non-prestrained specimens

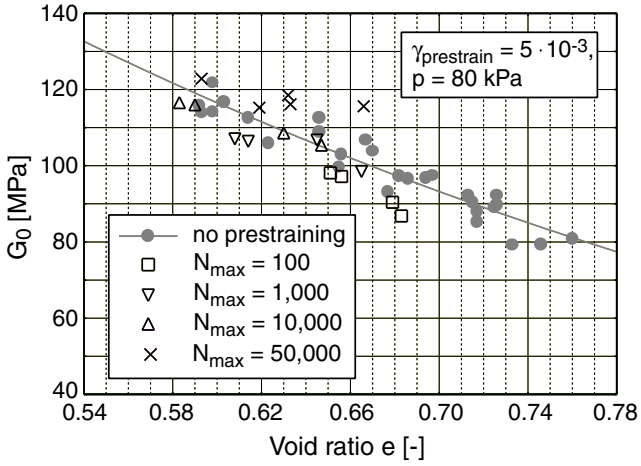

b) Change of void ratio due to prestraining

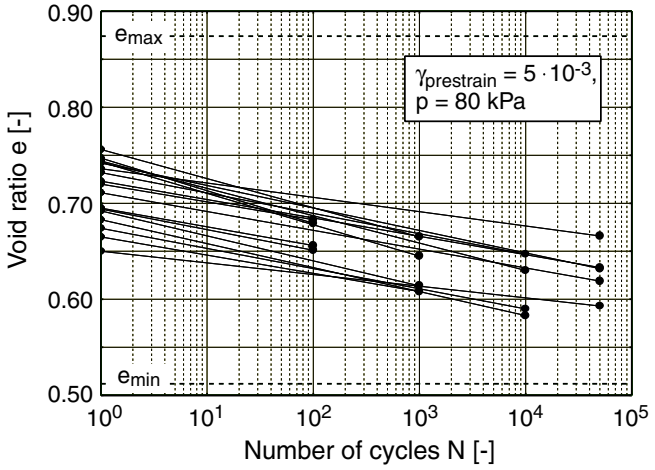

c) Change of G_0 due to prestraining

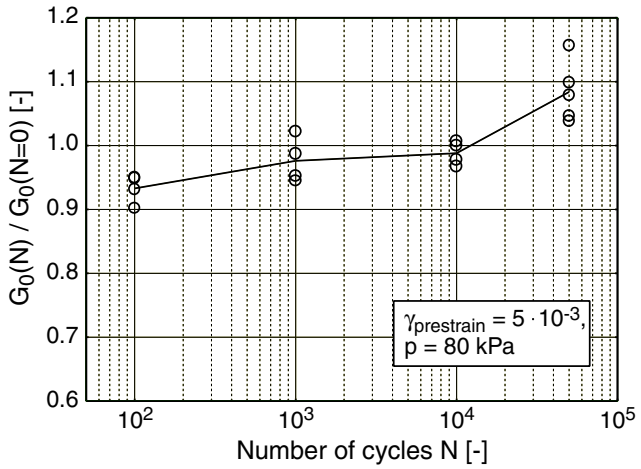

d) Curves $G(\gamma)$ after prestraining

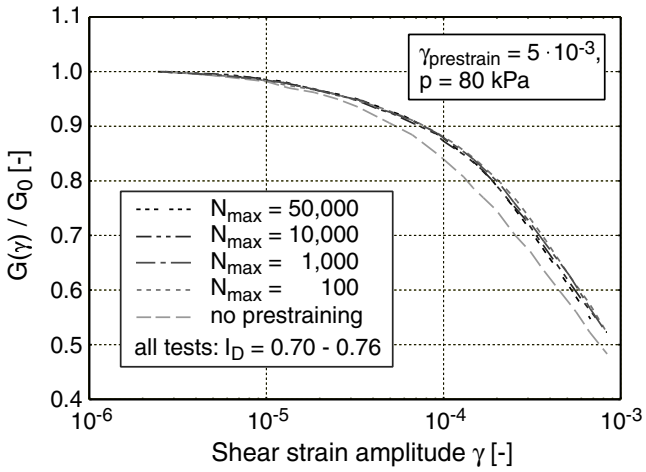

e) Curves $D(\gamma)$ due to prestraining

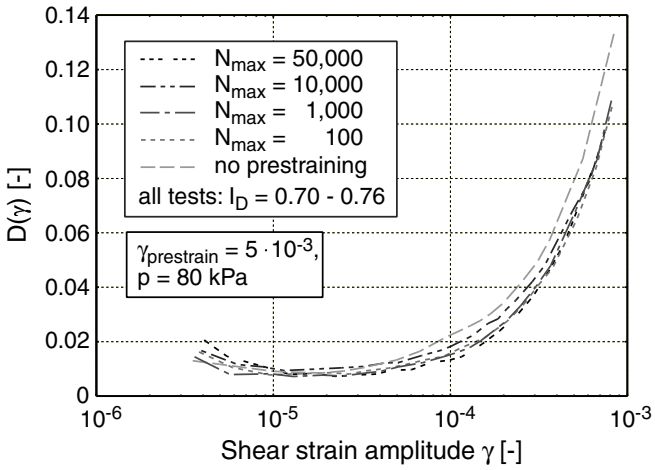

Fig. 20: *Results of tests with cyclic prestraining in the torsional shear device with a prestraining amplitude* $\gamma_{prestrain} = 5 \cdot 10^{-3}$, *tests on medium sand 2*

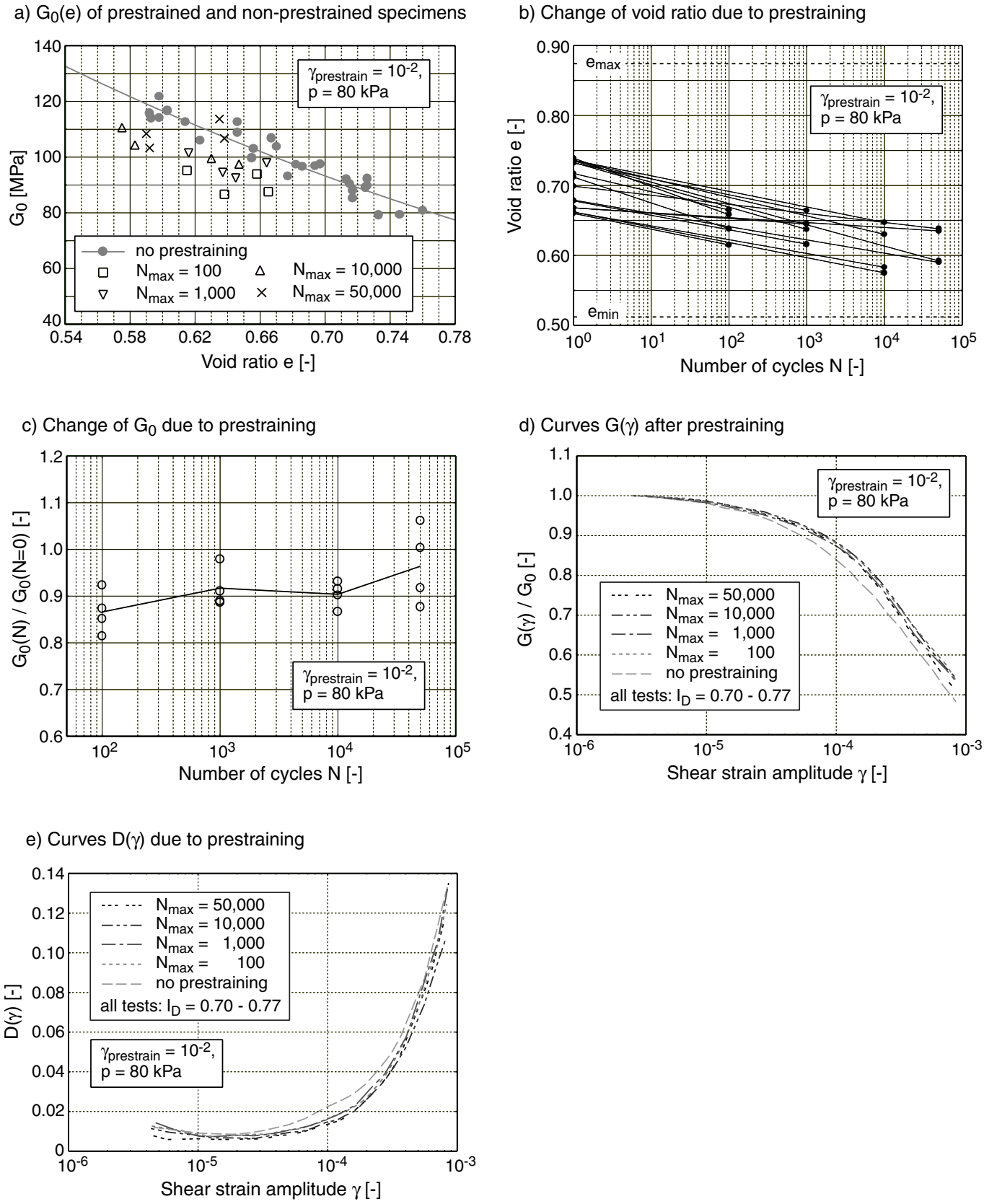

Fig. 21: *Results of tests with cyclic prestraining in the torsional shear device with a prestraining amplitude* $\gamma_{prestrain} = 10^{-2}$, *tests on medium sand 2*

calculated and are presented as the solid line in Fig. 20c). It can be concluded that small strain shear modulus G_0 was reduced somewhat during the first strain cycles. In the case of the amplitude $\gamma_{\text{prestrain}} = 5 \cdot 10^{-3}$ this reduction amounted approximately 7 % in average. This reduction of small strain shear modulus during the first strain cycles was also observed in the case of dynamic prestraining of hollow cylinder specimens of medium sand 2 in the RC device as presented in Figs. 18b) and 18d). With increasing number of applied strain cycles the normalized small strain shear modulus G_0 increased. The average small strain shear modulus of specimens prestrained with 50,000 cycles was approximately 9 % higher than the corresponding value of a non-prestrained specimen.

Fig. 20b) shows the change of void ratio due to prestraining. Since only the void ratios before and after prestraining could be determined and no data concerning the development of void ratio during prestraining were available, the initial void ratio and the void ratio after prestraining are connected linearly in this semilogarithmic diagram in order to present the tendency of void ratio change. Maximum and minimum void ratios of the used sand are marked as dashed lines. It can be stated that the volume of the specimens was reduced significantly due to prestraining and thus the fabric of the sand should have changed too. Although the fabric of the sand is drastically changed by prestraining the small strain shear modulus G_0 is moderately affected only. Fig. 20d) presents some representative modulus degradation curves $G(\gamma)/G_0$ of specimens prestrained with different maximum number of strain cycles and compares those curves with a representative curve of the non-prestrained specimens. The curves shown in this diagram are taken from tests with nearly identical relative density after prestraining. It can be seen from Fig. 20d) that the modulus decay versus strain was slightly smaller in the case of the prestrained specimens up to a shear strain amplitude of $\gamma = 2 \cdot 10^{-4}$. At higher shear strains the modulus degradation curves of the non-prestrained and the prestrained curves were nearly parallel. This observation coincides with the results of the tests with dynamic prestraining in the RC device where the modulus degradation curves during re-increasing of shear strain amplitude were more flat than the curves of the first increase of shear strain amplitude. No significant difference could be observed in the modulus degradation curves concerning the applied number of cycles. In Fig. 20e) the curves of damping ratio $D(\gamma)$ for different $N_{\max}$ are shown. It can be seen that the values of the prestrained specimens were slightly lower than the corresponding ones of the non-prestrained specimens. This is especially true for shear strains higher than $\gamma = 10^{-4}$. However this difference is not considered to be substantial.

In Figs. 21a) up to 21e) the experimental data of the tests with a prestraining amplitude of $\gamma_{\text{prestrain}} = 10^{-2}$ are presented. The tendencies in these tests were the same as pointed out in the diagrams of the tests with $\gamma_{\text{prestrain}} = 5 \cdot 10^{-3}$. The reduction of small strain shear modulus G_0 due to the first loading cycles was larger than in the tests with the lower prestraining amplitude. Although the scatter of test data in the tests with amplitude $\gamma_{\text{prestrain}} = 10^{-2}$ was larger than in the tests with $\gamma_{\text{prestrain}} = 5 \cdot 10^{-3}$, it can be stated that the percent increase of small strain shear modulus between 100 and 50,000 cycles did not differ remarkable between the two studied prestraining amplitudes. Thus, even if specimens were subjected to strain cycles with relatively high amplitudes only moderate changes of small strain shear moduli G_0 could be observed. Concerning the measured curves $G(\gamma)/G_0$ and $D(\gamma)$ for this case the observations pointed out for the tests with prestraining amplitude $\gamma_{\text{prestrain}} = 5 \cdot 10^{-3}$ hold true.

8 Summary and conclusions

The results of the performed tests can be summarized as follows:

a) Dynamic prestraining of specimens with full cross section in the resonant column device only moderately affected small strain shear modulus of dry sand. A reduction of small strain shear modulus due to the first strain cycles could be observed. During the following strain cycles a slight increase of small strain stiffness could be measured.

b) From similar tests on hollow cylinder specimens prestrained dynamically in the resonant column device it could be concluded that the specimen's cross section and thus the homogeneity of the distribution of shear strains does not play an important role concerning the development of small strain stiffness due to prestraining. No significant difference on the experimental results between full and hollow cylinder specimens could be detected.

c) Hollow cylinder specimens prestrained cyclically with higher shear strain amplitudes ($\gamma_{\text{prestrain}} = 5 \cdot 10^{-3}$ and $\gamma_{\text{prestrain}} = 10^{-2}$) showed similar tendencies as the specimens prestrained dynamically with lower prestraining amplitudes. Small strain shear modulus was reduced during the first strain cycles and then increased slightly. Although relatively high amplitudes were applied to the specimens and the volume of the specimen was significantly reduced in this cyclic test series the increase of small strain shear modulus in comparison with the value of the non-prestrained specimens did not exceed 10 % during 50,000 cycles. Large increases

of small strain shear modulus as documented by Drnevich and Richart [2] could not be observed.

d) A signature of previbration history was observed. A plateau in the curves of shear modulus $G(\gamma)$ and damping ratio $D(\gamma)$ at the prestraining amplitude $\gamma_{\text{prestrain}}$ was developed due to prestraining. A procedure has been proposed in order to describe the size of the received plateaus by the determination of a plateau area. The plateaus became more pronounced with increasing number of applied strain cycles. Thus, the sand remembers its previbration amplitude and the number of applied cycles. The signature of strain history was destroyed to some extend by a change of confining pressure after prestraining. If packages of strain cycles with different prestraining amplitudes are applied the succession of these packages plays an important role. It has to be stated that a development of a previbration signature could be even observed at strains lower than the assumed elastic threshold strain $\gamma = 10^{-4}$.

The purpose of this investigation was to study if the application of a cyclic strain history leads to measurable increases of small strain shear stiffness of sand. As stated above the changes were only moderate. Thus, small strain shear modulus of a sand cannot be correlated with its cyclic strain history or the soil fabric resulting from this history.

Acknowledgements

This study was conducted as part of the subproject A8 "Influence of the fabric changes in soil on the lifetime of structures", which is supported by the German Research Council (DFG) within the scientific collaborative centre SFB 398 "Lifetime oriented design concepts". The authors are deeply indepted for this financial support, which is greatly acknowledged herewith.

References

[1] Wichtmann T, Triantafyllidis T. Influence of a cyclic and dynamic loading history on dynamic properties of dry sand, part II: cyclic axial preloading. Soil Dynamics and Earthquake Engineering (submitted to publication)

[2] Drnevich V P, Richart F E. Dynamic prestraining of dry sand. Journal of the Soil Mechanics and Foundation Division, ASCE, 1970; 96(SM2):453-467

[3] Shen C K, Li X S, Gu Y Z. Microcomputer based free torsional vibration test. Journal of Geotechnical Engineering, ASCE, 1985; 111(8):971-986

[4] Alarcon-Guzman A, Chameau J L, Leonardos G A, Frost J D. Shear modulus and cyclic undrained behavior of sands. Soils and Foundations 1989; 29(4):105-119

[5] Lo Presti D C F, Pallara O, Lancellotta R, Armandi M, Maniscalco R. Monotonic and cyclic loading behaviour of two sands at small strains. Geotechnical Testing Journal 1993; 16(4):409-424

[6] Li X S, Yang W L, Chen C K, Wang W C. Energy-injecting virtual mass resonant column system. Journal of Geotechnical and Geoenvironmental Engineering, ASCE, 1998; 124(5):428-438

[7] Li X S, Yang W L. Effects of vibration history on modulus and damping of dry sand. Journal of Geotechnical and Geoenvironmental Engineering, ASCE, 1998; 124(11):1071-1081

[8] Li X S, Cai Z Y. Effects of low-number previbration cycles on dynamic properties of dry sand. Journal of Geotechnical and Geoenvironmental Engineering, ASCE, 1999; 125(11):979-987

[9] Tatsuoka F, Iwasaki T, Yoshida S, Fukushima S, Sudo H. Shear modulus and damping by drained tests on clean sand specimen reconstitued by various methods. Soils and Foundations 1979; 19(1):39-54

[10] Hertz H. Über die Berührung fester elastischer Körper. Journal für reine und angewandte Mathematik 1881; 92:156-171

[11] Goddard J D. Nonlinear elasticity and pressure-dependent wave speeds in granular media. Proceedings of the Royal Society of London 1990; 430:105-131

[12] Coppersmith S N, Liu C-H, Majumdar S, Narayan O, Witten T A. A model for force fluctuations in bead packs. Physical Reviews E. 1996; 53:4673:4685

[13] Triantafyllidis T, Niemunis A. Open questions concerning modeling of cyclic behavior of non-cohesive soils (in German). Issue No 32, Schriftenreihe des Instituts für Grundbau und Bodenmechanik, Ruhr-Universität Bochum, 2000

[14] Wichtmann T, Sonntag T, Triantafyllidis T. On the memory capacity of sand under cyclic loading (in German). Bautechnik 2001; 78(12):852-865

[15] Wichtmann T. Prognosis of densification potential of sand due to cyclic loading (in German). Diploma thesis. Institute for Soil Mechanics and Foundation Engineering, Ruhr-University Bochum, December 2000

[16] Yu P, Richart F E. Stress ratio effects on shear modulus of dry sands. Journal of Geotechnical Engineering, ASCE, 1984; 110(3):331-345

[17] Bellotti R, Jamiolkowski M, Lo Presti D C F, O'Neill D A. Anisotropy of small strain stiffness in Ticino sand. Géotechnique 1996; 46(1):115-131

[18] Afifi S S, Woods R D. Long-term pressure effects on shear modulus of soils. Journal of the Soil Mechanics and Foundations Division, ASCE, 1971; 97(SM10):1445-1460

[19] Afifi S S, Richart F E. Stress-history effects on shear modulus of soils. Soils and Foundations 1973; 13(1):77-95

[20] Baxter C D P. An experimental study on the aging of sands. PhD thesis. Faculty of the Virginia Polytechnic Institute and State University, July 1999

[21] Benedetto H D, Tatsuoka F, Ishihara M. Time-dependent shear deformation characteristics of sand and their constitutive modelling. Soils and Foundations 2002; 42(2): 1-22

[22] Chen Y C, Ishibashi I, Jenkins J T. Dynamic shear modulus and fabric: part II, depositional and induced anisotropy. Géotechnique 1988; 38(1): 25-32

[23] Hardin B O, Drnevich V P. Shear modulus and damping in soils: measurement and parameter effects. Journal of the Soil Mechanics and Foundations Division, ASCE, 1972; 98(SM6): 603-624

[24] Hardin B O, Drnevich V P. Shear modulus and damping in soils: design equations and curves. Journal of the Soil Mechanics and Foundations Division, ASCE, 1972; 98(SM7): 667-692

[25] Ishibashi I, Chen Y C Jenkins J T. Dynamic shear modulus and fabric: partII, stress reversal. Géotechnique 1988; 38(1): 33-37

[26] Iwasaki T, Tatsuoka F, Takagi Y. Shear moduli of sands under cyclic torsional shear loading. Soils and Foundations 1978; 18(1): 39-56

[27] Ray R P, Woods R D. Modulus and damping due to uniform and variable cyclic loading. Journal of Geotechnical Engineering, ASCE, 1988; 114(8): 861-876

[28] Richart F E, Hall J R, Woods R D. Vibrations of Soils and Foundations. New Yersey: Prentice-Hall, 1970

[29] Roesler S K. Anisotropic shear modulus due to stress anisotropy. Journal of the Geotechnical Engineering Division, ASCE, 1979; 105(GT7): 871-880

[30] Vucetic M. Cyclic threshold shear strain in soils. Journal of Geotechnical Engineering, ASCE, 1994; 120(12):2208-2228